INTERNATIONAL SCIENTIFIC JOURNAL

MECHANIZATION IN AGRICULTURE & CONSERVING OF THE RESOURCES



Issue 3
2023

Year LXIX, ISSN print:2603-3704, ISSN web 2603-3712

SCIENTIFIC TECHNICAL UNION OF MECHANICAL ENGINEERING
BULGARIAN ASSOCIATION OF MECHANIZATION IN AGRICULTURE

PUBLISHERS

SCIENTIFIC-TECHNICAL UNION OF MECHANICAL ENGINEERING "INDUSTRY-4.0"
BUGLARINA ASSOTIOATION OF AGRICULTURAL MACHINERY

ISSN (PRINT) 2603-3704, ISSN (ONLINE) 2603-3712

YEAR LXIX ISSUE 3 / 2023

EDITORIAL BOARD

Chief Editor: Prof. Dr. eng Miho Mihov
Responsible secretary: Corresp. Memb. Prof. D.Sc. Hristo Beloev

MEMBERS:
Acad. D.Sc. Jemal Katsitadze – Georgia
Acad. D.Sc. Sayaкhat Nukeshev - Kazakhstan
Acad. D.Sc. Volodymyr Bulgakov – Ukraine
Acad. D.Sc.Valeriy Adamchuk – Ukraine
Prof. Abdullah Sessiz - Turkey
Prof. Abdulrahman Al-soqeer - Saudi Arabia
Prof. Alexander Tokarev - Russia
Prof. Alexey Vassilev - Russia
Assoc.Prof. Angel Trifonov - Bulgaria
Prof. Anupam Kumar Nema - India
Prof. Ayrat Valiev - Russia
Prof. Barbro Ulén - Sweden
Prof. Carmen Puia - Romania
Prof. Cheslav Vashkievich - Poland
Prof.Cumhur Aydinalp - Turkey
Prof. Daisuke Higaki - Japan
Prof. Davor Romic - Croatia
Prof. Domenico Pessina - Italy
Dr. Finn Plauborg - Denmark
Assoc.Prof. Ganka Baeva - Bulgaria
Assoc. Prof. Dr. Mariusz Szymanek - Poland
Prof. Georgi Tassev - Bulgaria
Prof. Haiyan Huang - China
Prof. Hoang Thai Dai - Vietnam
Prof. Iliya Malinov – Bulgaria
Eng. Ivan Opacak - Croatia
Prof. PhD Iurie Melnic - Moldova
Assoc.Prof. Ivan Ivanov - Bulgaria
Prof. Jan Szczepaniak - Poland
Prof. Komil Muminov - Uzbekistan
Prof. Krassimira Georgieva - Bulgaria
Prof. Maja Manojlović - Serbia
Prof. Mihail Iliev - Bulgaria
Prof. Mohammad Salem Al-Hwaiti - Jordan
Prof. Papamichail Dimitris - Greece
Prof. Pavel Tlustos - Czech Republic
Prof. Plamen Kangalov - Bulgaria
Prof. Ralph Meissner - Germany
Prof. Rossen Ivanov - Bulgaria
Prof. Svetla Rousseva - Bulgaria
Prof. Tadeusz Pawłowski - Poland
Prof. Tamara Persikova - Belarus
Prof. Valentina Kundius - Russia
Prof. Wojciech Tanaś - Poland
Prof. Yerbol Sarkynov - Kazakhstan
Prof. Zdenko Tkach - Slovakia
Prof. Zinta Gaile - Latvia
Prof. Zivko Davchev - Macedonia

The journal "MECHANIZATION IN AGRICULTURE & CONSERVING OF THE RESOURCES " is continuer of the journals "Mechanized farming" (1948-1957), "Mechanization and electrification of agriculture" (1959-1980) and "Mechanization of agriculture " (1981-1991)

108, Rakovski Str., 1000 Sofia, Bulgaria
tel. (+359 2) 987 72 90, tel./fax (+359 2) 986 22 40,
office@stumejournals.com
WWW.STUMEJOURNALS.COM

C O N T E N T S

MECHANIZATION IN AGRICULTURE

Experimental study of the transportation process bulk materials of agro-industrial production by pneumatic auger conveyor
Volodymyr Bulgakov, Valerii Adamchuk, Volodymyr Nadykto, Oleksandra Trokhaniak; Ivan Beloev 76

Combined unit of small mechanization, experimental calculations and its advantages
Giorgi Kutelia, Otar Karchava, Vladimir Miruashvili. Avto Tsverikmazashvili 79

Assessment of stability of a forest tractor with a hydraulic arm
Ján Diţo, Miroslav Blatnický, Vadym Ishchuk, Denis Molnár 82

Experimental study of the driving resistance of a harrow with screw working bodies
Volodymyr Bulgakov, Ivan Holovach, Mykola Klendii, Oleksandra Trokhaniak, Yevhen Ihnatiev, Olha Dubrovina 86

Design and strength analysis of the end carriage beam for the single girder bridge crane of a 500 kg load capacity
Denis Molnár, Miroslav Blatnický, Dalibor Barta, Juraj Grenčík 89

Implementation of digital penetrometer S600 skokagro in the technology of precision and digital agriculture
Anatolii Kobets, Oleksii Derkach, Viktor Aulin, Dmytro Makarenko, Oleh Serhiienko 95

Research and justification of automated monitoring of the microclimate of a farmer's greenhouse
Atihanov Aybek Kashkymbaevich, Bekaidarova Bakytkul Nurlybekovna 98

CONSERVING OF THE RESOURCES

Comparison of tillage technologies in relation to changes in soil properties using soil biostimulation
Pavol Findura, Miroslav Prístavka, Hristo Beloev, Plamen Kangalov, Mitko Nikolov 102

Methodical approach to determine the gamma-percentage resource of aggregates and units of forklift trucks
Ivan Bitunski, Miho Mihov 105

Characterization of lettuce germplasm (*Lactuca sativa* L.) stored in the Genetic Bank of Albania
Valbona Hobdari 109

Experimental study of the transportation process bulk materials of agro-industrial production by pneumatic auger conveyor

Volodymyr Bulgakov[1]; Valerii Adamchuk[2]; Volodymyr Nadykto[3]; Oleksandra Trokhaniak[1]; Ivan Beloev[4]

[1]National University of Life and Environmental Sciences of Ukraine, Kyiv, Ukraine
[2]Institute of Mechanics and Automation of Agricultural Production
of the National Academy of Agrarian Sciences of Ukraine, Ukraine
[3]Dmytro Motornyi Tavria State Agrotechnological University, Ukraine
[4]«Angel Kanchev» University of Ruse, Bulgaria
E-mail: *vbulgakov@meta.ua

Abstract. *The article presents the developed experimental installation of a pneumatic screw conveyor and a research methodology for determining the power indicators that arise when moving bulk materials from the effects of air pressure and the volume of various types of bulk materials. Graphic dependences of the moving cargo effort on air pressure and the action of moving different bulk materials on their volume at constant air pressure are built. The dependences of the productivity of the pneumatic screw conveyor on the change in the area of the hopper opening, the rotational speed of the screw feeder and the value of the working air pressure in the technological line are established.*

KEYWORDS: *CONVEYOR, BULK MATERIAL, SCREW FEEDER, AIR PRESSURE*

1. Introduction

To transport bulk materials of agro-industrial production with minimal damage, combinations of mechanical supply of material by a screw feeder with recharge by a jet of compressed air are often used. In agricultural production enterprises for bulk materials transportation, high-pressure pneumatic conveying equipment of the injection type is widely used. However, in many cases, it turned out to be ineffective since it is expensive to maintain, structurally complex, and requires cyclones to capture material particles from the dust cloud of the flow.

Screw conveyors have found wide use in the layout of machines for reloading or moving bulk materials due to their simplicity of design, maintenance and the ability to load and unload material anywhere in the process line. Based on the analysis of literary and patent sources for the designs of working bodies and methods for transporting bulk materials in closed casings along straight and curved routes [1-4], it was found that they satisfy some of the requirements for the quality of the technological process.

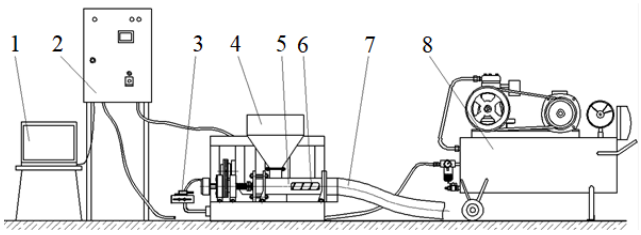
However, at the same time, issues related to increasing the productivity of conveyors, reducing energy costs for the implementation of the technological process, the reliability of working bodies, minimizing damage to transported bulk materials, etc., have not been fully resolved [5, 6]. Thus, among the urgent tasks of agricultural production, it is important to develop and justify the rational parameters of pneumatic screw conveyors that ensure the efficient movement of grain materials.

The work aims to increase the efficiency of screw conveyors, which ensure the movement of bulk materials along technological routes of various spatial configurations using mechanical material supply through a screw feeder and an additional increase in the flow of bulk material with compressed air.

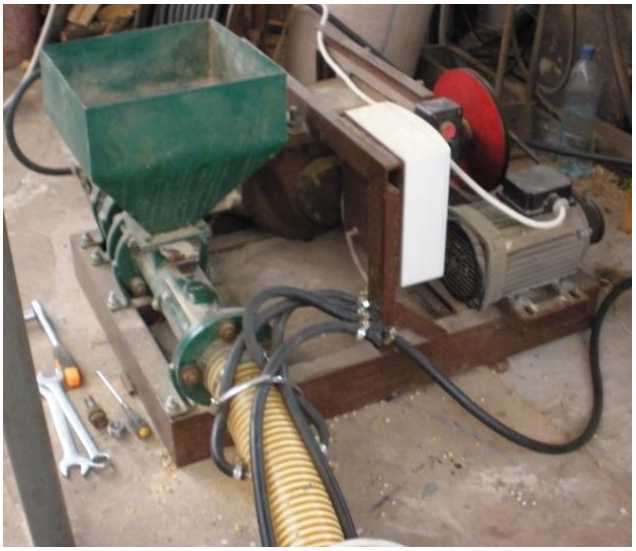
2. Materials and Methods

To conduct experimental studies, an installation of a pneumatic screw conveyor was developed with replenishment of the transport flow with an air jet (Fig.1).

Pneumatic auger conveyor works as follows. Bulk material through hopper 4 enters the body of conveyor 5 on auger 6, which rotates and moves this material to the unloading area. When an overload occurs due to accumulating a certain dose of bulk material in the working chamber of the conveyor body 5, screw 6 is displaced opposite to the direction of bulk material transportation and compresses the spring.



a



b

Figure 1*. Diagram (a) and general view (b) of the pneumatic screw conveyor experimental installation:*
1 - computer; 2 - "Altivar-71"; 3 - pneumatic distributor;
4 - bunker; 5 – conveyor body; 6 - auger; 7 - flexible transport sleeve; 8 – compressor

In this case, the pressure disk interacts with the pneumatic distributor 3, which admits high-pressure air from the pneumatic system. Air enters the central hole of the splined shaft. This leads to the "liquefaction" of the bulk material mass and its further transportation. At the same time, a pneumatic valve is automatically turned on, which closes the exit zone from the bunker and makes the working chamber of the conveyor body airtight.

When the material is moved, the axial pressure on screw 6 decreases, and under the action of the compression spring, it is withdrawn in the direction of the bulk material transportation. This leads to the movement of the pressure plate, which turns off

the pneumatic valve 3 and blocks the air from the pneumatic system.

Fig. 1b shows a general view of the pilot plant of the pneumatic screw conveyor. One of its main nodes is the mechanism for switching on the pneumatic distributor (Fig. 2). This mechanism aims to replace the mechanical action on the transport material with a pneumatic one, provided that certain critical (limiting) conditions are met. This condition is the mass of transported bulk material. When a critical mass is accumulated in the feeder housing, the pneumatic distributor is switched on (not shown in the figure).

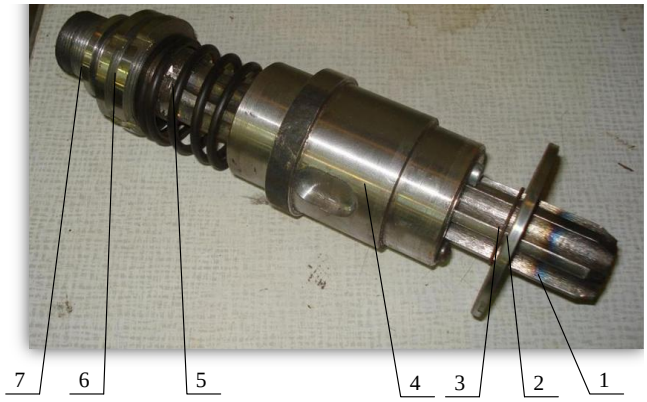


Figure 2*. The mechanism of the pneumatic distributor starting:*
1 - splined shaft with semicircular splined grooves;
2 - contact washer; 3 - retaining ring;
4 - slotted sleeve; 5– spring; 6 - bushing;
7 - lock nuts

The return movement of the sleeve is provided through a compression spring. The latter is the regulator of the limit force of the mechanism actuation. The sensitivity of the mechanism is ensured by using a ball spline connection. This type of connection transmits a slightly lower torque with less axial movement of the connecting elements. At the same time, it works smoothly, without jamming and bruising, and ensures the absence of distortions.

Fig. 3 shows the connection of the mechanism for switching on the pneumatic distributor with the switch of the three-line type P-RKI.4. To determine the power parameters of the bulk materials transportation process, an Altivar-71 frequency converter with Power Suite v.2.5.0 software was used.

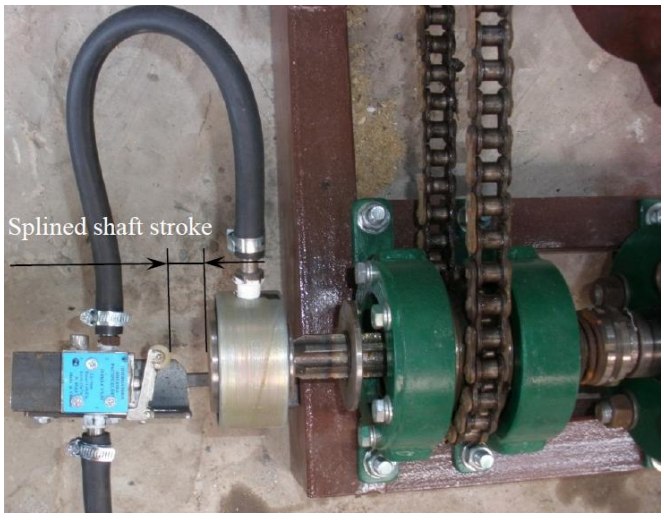


Figure 3. *Connection of the mechanism for switching on the pneumatic distributor with a three-line type switch P-RKZ.4*

The Altivar 71 system is connected to the network and the computer. When the desired speed is set using a computer through the Altivar 71 system, the screw feeder shaft rotates with the set parameters. Changing the latter makes it possible to establish their influence on the torque T and engine power N depending on the rotational speed of the working body $\boldsymbol{n}$ when it is overloaded. In experimental studies, such bulk materials as wheat, bran and sawdust were used.

3. Results and discussions

Based on the results of experimental studies, graphical dependencies were built: i) the effort of moving the load on air pressure (Fig. 4); ii) the force of movement of bulk materials from their volume at constant air pressure $P = 0.6$ N·mm^{-2} (Fig. 5).

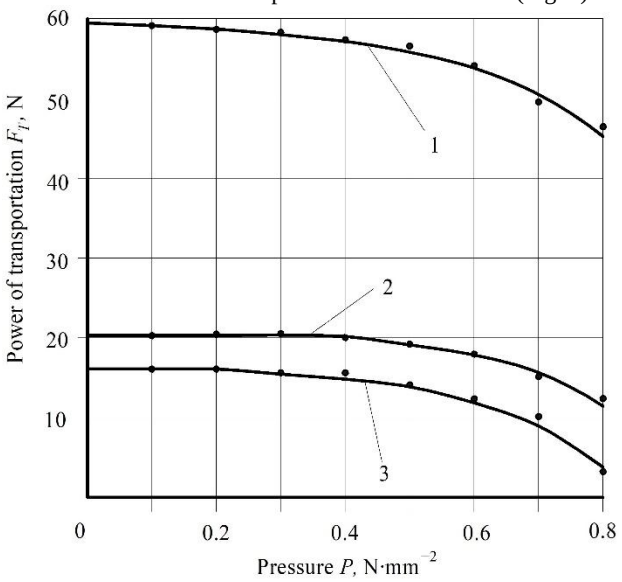


Figure 4. *Dependences on bulk material transportation force on air pressure:*
1 - wheat; 2 - sawdust; 3 - bran

From the analysis of the graphs, it follows that the force of transporting bulk materials decreases with an increase in air pressure P in the pneumatic system (Fig. 4) and increases with an increase in volume V of bulk materials per linear meter (Fig. 5). The bulk density of the bulk material also has a significant effect on the magnitude of the force F_T.

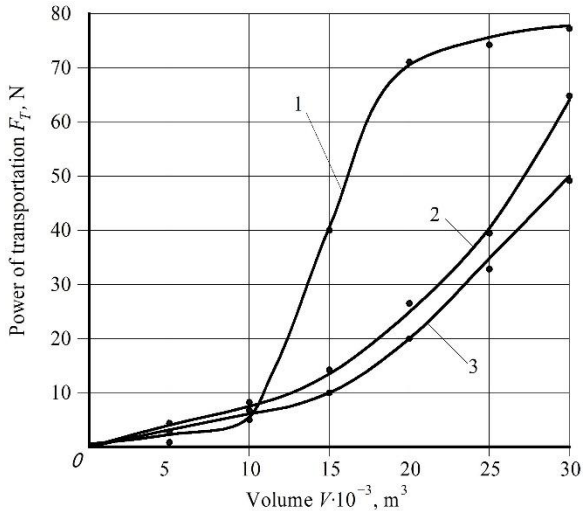


Figure 5. *Dependences of the force of moving the material per linear meter F_T on volume V of bulk material:*
1 - wheat; 2 - sawdust; 3 - bran

According to the results of experimental studies, the following dependences were obtained: i) the performance of the pneumatic screw conveyor on the change in the area of the hopper outlet opening $12 \le S_c \le 36$ cm^2; ii) feeder speeds $150 \le n \le 450$ rpm; iii) the value of the working air pressure $0.2 \le P \le 0.3$ N·mm^{-2} in the technological line. These dependencies are presented as a functional $Q = f(S_c, P)$ at n = 300 rpm (Fig. 6) and a functional $Q = f(n, P)$ at $S_c = 24$ cm^2 (Fig. 7).

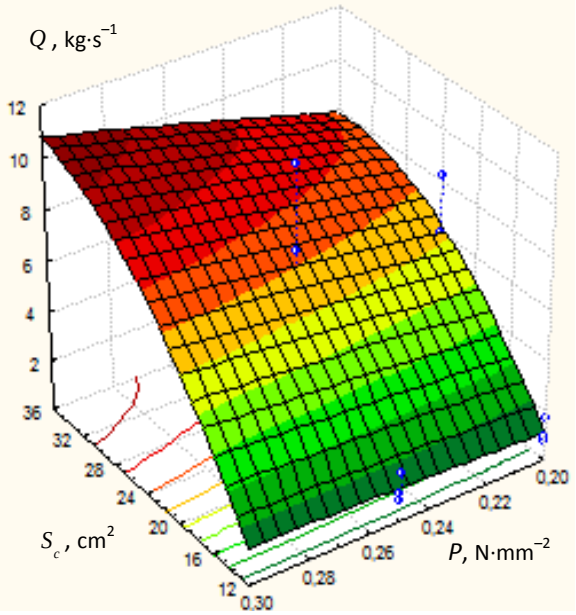


Figure 6. *Pneumatic conveyor performance response surface as a functional Q = f (Sc, P) at n = 300 rpm*

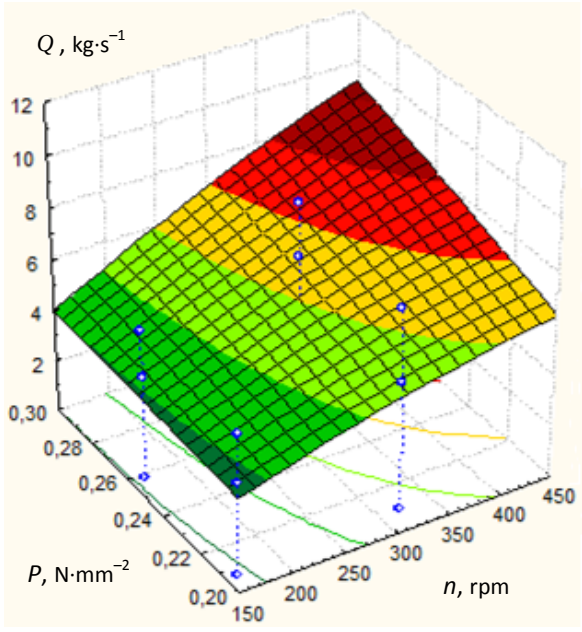


Figure 7. *Pneumatic conveyor performance response surface as a functional Q = f (n, P) at S_c = 24 cm^2*

The analysis of the response surfaces and their two-dimensional sections shows that the performance Q of the pneumatic screw conveyor increases with the increase in the acting factors and is approximately in the range of 2…11 kg·s^{-1} depending on their change, but the influence of each element has a different character.

The most significant influence on the nature of the change in the productivity of the pneumatic screw conveyor Q is exerted by the screw speed n and the outlet area S_c. In this case, a significant increase in Q occurs with an increase in the value of the corresponding factors $S_c \ge 24$ cm^2 and $n \ge 300$ rpm.

4. Conclusion

The article presents an experimental installation of a pneumatic screw conveyor and a methodology for conducting experimental laboratory studies to determine the power indicators for the movement of bulk materials of agro-industrial production from the effects of air pressure and the volume of various types of materials. Based on the results of the experimental studies, graphical dependences of the load-displacement force on air pressure and the displacement force of different bulk materials on their volume at a constant air pressure P = 0.6 N·mm^{-2} were plotted. It has been established that the transportation force of bulk materials decreases with an increase in air pressure P in the pneumatic system and increases with an increase in volume V of bulk materials per linear meter.

Based on the manufactured installation of a pneumatic screw conveyor feeding the material flow with air jets, the productivity dependences of the pneumatic screw conveyor on changes in the area of the hopper opening, the screw feeder speed and the value of the working air pressure in the technological line were established.

An analysis of experimental studies results showed that the productivity Q of a pneumatic screw conveyor increases with an increase in operating factors and is approximately in the range of 2…11 kg·s^{-1}. The most significant influence on the nature of the change in productivity Q is exerted by the screw speed n and the outlet area S_c. At the same time, a significant increase in Q occurs with an increase in the value of the corresponding factors $S_c \ge 24$ cm^2 and $n \ge 300$ rpm.

The results of experimental studies can be used in developing industrial designs of pneumatic auger conveyors for agro-industrial production.

5. References

1. Bulgakov, V., Trokhaniak, O., Klendii, M., Ivanovs, S., & Dukulis, I. Research on the Impact of the Operating Modes and Main Design Parameters on the Efficiency of the Machine for Preparing and Packing Slaked Lime. – INMATEH: Agricultural Engineering, vol. 67. no. 2, 2022, pp. 323-330.

2. Olt, J., Bulgakov, V., Trokhaniak, O., Klendii, M., Gadzalo, I. A., Ptashnik, M., & Tkachenko, M. Harrow with screw-type operating tools: Optimization of design and process parameters. – Agronomy Research, vol. 20, no. 4, 2022, pp. 751-763.

3. Hevko R. B., Klendiy M. B., Klendiy O. M. Investigation of a transfer branch of a flexible screw conveyer. – INMATEH: Agricultural engineering, vol. 48, no. 1, 2016, pp. 29-34.

4. Lech M. Mass flow rate measurement in vertical pneumatic conveying of solid. – Powder Technology, vol. 114, Issues 1–3, 2001, pp. 55-58.

5. Bulgakov V., Olt J., Ivanovs S., Trokhaniak O., Gadzalo Ja., Adamchuk V., Chernovol M., Pascuzzi S., Santoro F., Arak M. Research of a contact stresses in swivel elements of flexible shaft in screw conveyor for transportation of agricultural materials. – Estonian Academic Agricultural Society. Agraarteadus, vol. 33, no. 1, 2022, pp. 67-73. doi:10.15159/jas.22.12.

6. Hevko R. B., Rozum R. I., Klendiy O. M. Development of design and investigation of operation processes of loading pipes of screw conveyors. – INMATEH: Agricultural engineering, vol.50, no. 3, 2016, pp. 89-94.

Combined unit of small mechanization, experimental calculations and its advantages

Giorgi Kutelia[1]. Otar Karchava[1]. Vladimir Miruashvili[2]. Avto Tsverikmazashvili[2]
Scientific-Research Center of Agriculture of Georgia. Tbilisi, Georgia.

Abstract: *The article discusses the designs of small-scale mechanization technical means that are used in Georgia, namely, agricultural machinery installed on moto blocks, the scale and advantages of their use compared to powerful machinery and based on a patent (No. AP 2020 15395), completely new combined aggregate is presented as part of a moto block, which is currently in demand in the context of the development of modern technologies for growing crops on the market. In particular, in small areas and greenhouses. The article proposes a constructive description of the presented combined aggregate and the principles of its operation. Theoretical waste was also carried out using similarity and dimensionality theories. The functional relationship between the optimization parameters and the operating factors is determined and the regression equation is selected, on the basis of which the optimal operating modes are determined.*
KEY WORDS: *AGRICULTURE, MECHANIZATION, MOTO BLOCK, AGGREGATE, NEW TECHNOLOGIES.*

Introduction

To perform the operations necessary for the complex mechanization of the care and cultivation of agricultural crops, both mobile and technical means of small-scale mechanization are used - moto blocks with loops. Their use is especially effective for regions where agricultural areas are small in contour and located in mountainous conditions. For these regions, a combined resource-saving agricultural aggregate based on a moto block for the formation of furrows in the soil and mulching is proposed.

The combined aggregate allows you to loosen the soil using tillage machines with active working bodies (milling cutters), form a furrow, lay a drip irrigation system, lay plastic mulch, cover it with soil and make holes on the laid plastic mulch, in one pass with low energy consumption. The proposed aggregate is a significant innovation both in terms of scientific and practical application, it will complement the untapped market segment in terms of the use of equipment in the agricultural sector, where it is not possible to use heavy machinery. This aggregate will be in great demand in small and closed ground areas (greenhouses), among crop producers growing vegetables, melons and small-fruited crops, which are considered by the Georgian state as a priority in the agricultural sector.

The regions of Georgia are distinguished by many features, such as the location of agricultural land on the slopes, fragmented areas with a narrow contour, mountainous conditions, sloping terrain, high humidity, solar radiation, soil types and much more. Due to these circumstances, it is impossible to use heavy machinery on most of the arable land, therefore, the main work is done manually using technical means of small-scale mechanization.

According to the study, the total area of plots up to 1 ha is 12.7% of the total area of arable land, and the volume of plots from 1 to 5 ha is 19.3%. [1] It is in these areas that small farmers and peasants grow vegetables, melons and small-fruited crops. The above-mentioned small farmers and peasants are the main users of small-scale mechanization equipment.

Basic part

The machine for laying on the soil of plastic tape for mulching contains a frame, connected with the power tool, on which there are installed in sequence the tools for tillage and profiling of surface of furrows, a roll of plastic mulching tape, and soil fillers. The machine is additionally equipped with a drum with a drip irrigation pipe and a mulch tape perforator. Also, the drum with a drip irrigation pipe reeled on it is installed on the frame after the tool for profiling of furrow surface, which is a bow-shaped shield, and the soil-cultivating tool is made in the form of a rotary tiller with a horizontal shaft mounted on the front of the frame. Also, the power supply is a motoblocks, while the frame has supporting wheels, with the mulch tape perforator placed on the axle of support wheels and positioned between the mulch tape roll and the soil fillers. (Figures 1-2) shows the principle diagram of the proposed aggregate.

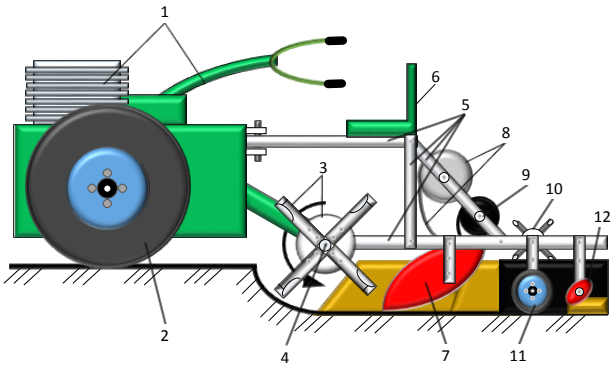


Fig-1

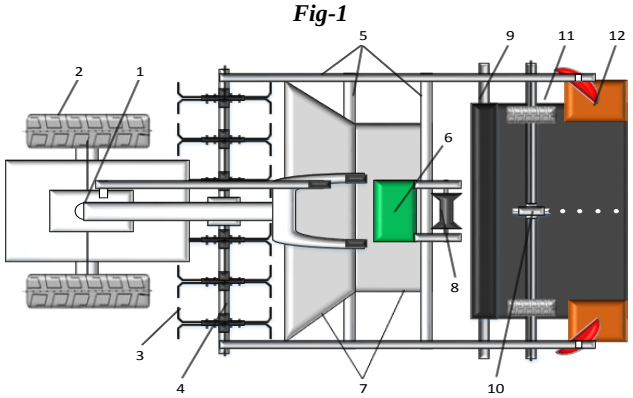


Fig-2. *Innovative combined unit for mulching soil on the basis of a motoblocks (fig-1) side view (fig-2) top view.*

The aggregate laying of plastic tape on soil for mulching contains the power tool - motoblocks 1 with drive wheels 2 to which frame 3 is connected. On the front part of frame 3, a soil cultivating tool is mounted, which is made in the form of rotary tiller 5 with horizontal shaft 4. The operator's seat 6 is attached to the upper side of frame 3. On the lower side of frame 3, after the rotary tiller 5, a tool for profiling the furrow surface is attached, which is a bow-shaped shield 7.After the mentioned tool 7 for profiling of furrow surface, a drum 8 with drip watering pipe reeled on it, the roll 9 of the mulching tape, the perforator of the mulching tape 10, and soil fillers 11 are mounted on the frame 3 in sequence. Frame 3 is equipped with support wheels 12. The perforator 10 of the mulching tape 9 is placed on the axle of the support wheels 12 and is located between the roll of mulch tape 9 and soil fillers 11.

The aggregate works as follows: after starting the engine of the motoblocks 1, the coupling (not shown in the drawings) of the drive wheels 2 and the rotary tiller 5 is turned on, as a result of which the two-wheel tractor 1 moves forward and the rotary tiller 5 starts working - cutting and loosening the soil layer. The layer of soil cut by the knives of the rotary tiller 5 is thrown back and meets the tool for profiling of furrow surface, which is a bow-shaped shield 7; its shape gives the soil layer cut by the rotary tiller 5 a certain direction and forms a furrow with a smooth surface. At the center of the profiles made by the rotary tiller 5 and the bow-shaped shield 7, a flexible drip irrigation pipe reeled on the drum is unreeled, then the pipe is covered with plastic mulch tape 9 from the roll 9 for

mulching. The support wheels 12 move on the edges of the mulch tape 9, and the perforator 10, rotating under the action of the axle of support wheels, in the same zone makes holes for planting of saplings, and the edges of the mulch tape 9 are covered by loose soil using soil fillers 11.[2].

The proposed aggregate for laying on the soil of mulching plastic tape is of simple construction, is characterized by low energy consumption, and allows to loosen a soil through a single pass of the motoblocks, to make furrows, unreel flexible drip irrigation pipe, to lay plastic mulch tape on furrows, to make pits for planting of saplings and cover the edges of the mulch tape with soil.[2-3].

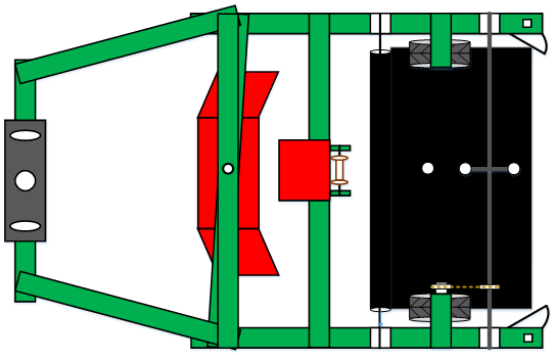


Fig.3 *Aggregate, top view prototype-1.*

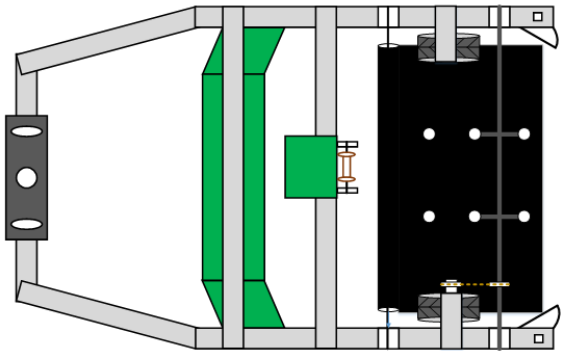


Fig.4 *Aggregate, top view prototype-2.*

Results of theoretical research

Theoretical studies have been carried out, using the theory of similarity and dimension. Present them.

The list of factors affecting the power of the tractor Table.1

№	The name of the optimization parameter and factors	Designation	The dimension in the system Si	Dimension, expressions by the symbols of quantities
1	power	N	Watt	L^2MT^{-3}
2	the speed of movement of the moto blocks	V	m/s	LT^{-1}
3	undercut resistance	P	Newton	LMT^{-2}
4	soil density	ρ	kg/m^3	ML^{-3}
5	radius of trimming machine	R	m	L
6	cutting height	h	m	L
7	cutting width	b	m	L

Functional connection between optimization parameter and the factors affecting on it have the following face:

$$N = f(V, \rho, P, R, h, b)$$

This dependence can be expressed as similarity criteria. Their number is determined by π - theorem of dimensional analysis.

$$r = N - n$$

$N -$ number of values, $n -$ number of main factors. These factors should be selected as follows, to determine the exponents of their dimensions differed from zero. subject to these requirements, as the main factors we accept - the speed of movement of the tractor – V, undercut resistance – P and stem density – ρ.

The dimensions of these quantities can be represented as follows:

$$[V] = LM^0T^{-1}$$
$$[P] = LMT^{-2}$$
$$[\rho] = L^{-3}MT^0$$

The determinant of the exponents of these quantities is equal to:

$$\Delta = \begin{vmatrix} 1 & 0 & -1 \\ 1 & 1 & -2 \\ -3 & 1 & 0 \end{vmatrix} = -2 \quad \neq 0$$

This means that the main factors are chosen correctly.

Number of similarity criteria:

$$r = N - n = 7 - 3 = 4$$

It is necessary to obtain characteristic similarity criteria:

$$\pi = N\, V^{\alpha}\, \rho^{\beta}\, P^{\gamma} = 1$$
$$\pi_1 = R\, V^{\alpha_1}\, \rho^{\beta_1}\, P^{\gamma_1} = 1$$
$$\pi_2 = h\, V^{\alpha_2}\, \rho^{\beta_2}\, P^{\gamma_2} = 1$$
$$\pi_3 = b\, V^{\alpha_3}\, \rho^{\beta_3}\, P^{\gamma_3} = 1$$

Where $\alpha_i,\ \beta_i,\ \gamma_i -$ Unknown features.

To π_i - similarity criteria have become dimensionless, the exponents should be as follows, to replace each variable with the appropriate combination M, L, T in the resulting expressions, the exponent of the basic dimension was equal to zero [4].

With this in mind, it is possible to obtain a defined similarity criterion:

$$N\, V^{\alpha}\, \rho^{\beta}\, P^{\gamma} = L^2MT^{-3}\, L^{\alpha}T^{-\alpha}\, L^{-3\beta}M^{\beta}\, L^{\gamma}M^{\gamma}T^{-2\gamma} = L^0M^0T^0 = 1$$

We obtain the following linear equations:

$$2 + \alpha - 3\beta + \gamma = 0$$
$$1 + \beta + \gamma = 0$$
$$-3 - \alpha - 2\gamma = 0$$

The solution of these equations gives:

$$\alpha = -1;\ \beta = -2;\ \gamma = -1$$

Accordingly, the defined criterion has the form:

$$\pi = \frac{N}{PV}$$

Analogically, we obtain the defining similarity criteria:

$$\pi_1 = RV\sqrt{\frac{P}{\rho}};\quad \pi_2 = hV\sqrt{\frac{P}{\rho}};\quad \pi_3 = bV\sqrt{\frac{P}{\rho}}.$$

Physical meaning of the obtained criteria following:

$$\frac{N}{PV}$$

quality criterion dimensionless engine power. the rest are technological criteria, similarity:

$RV\sqrt{\frac{P}{\rho}}$ - Defining criterion. radius of trimming machine;

$hV\sqrt{\frac{P}{\rho}}$ - Defining criterion. cutting height;

$bV\sqrt{\frac{P}{\rho}}$ - Defining criterion. cutting width.

The primary testing of the above-mentioned experimental aggregate is carried out in the field. Identification of some shortcomings beat the correction, these aggregates are ready for use in experiments. The received data will be processed to improve the reliability of resource-saving technologies using the theory of similarity and dimensions.

According to the formula, which was transformed by one of the authors**, Professor Otar Karchava**, there will be definitions of the technical and economic indicators of these aggregates.

$$E_{ha} = \frac{E_{hour}}{W_{hour}} = \frac{E_{am.hour} + E_{f.hour} + E_{lab.hour}}{W_{hour}} = \frac{1}{W_{hour}}\left(\frac{M_{tr}\, e_{tr}}{T_{tr}} + \frac{n\, M_{imp}\, e_{imp}}{T_{imp}} + \frac{N_{pow}\, k_{pow}\, g_{ind}\, e_{fuel}}{\gamma} + f_{op}\, e_{op}\right)$$

Where E_{hour} Is the total energy spent by the given technological unit for one hour in megajoules (mj/hour);

$E_{am.hour}$ - The energy spent by the given technological aggregate for one hour in megajoules on the creation and amortization of the technological aggregate (maintenance, repair, restoration) (mj/hour);

$E_{f.hour}$ - The energy spent by the fuel-oil materials of the given technological aggregate during one hour in megajoules (MJ/hr);

$E_{lab.hour}$ - The energy spent by the operator of the given technological aggregate during one hour in megajoules (MJ/hr);

M_{tr} and M_{imp} - Accordingly it is the masses of the tractor and technological machines kg;

n - Number of machines in the technological aggregate;

T_{tr} and T_{imp} - Car load in the period of moral depreciation hour;

e_{tr} *and* e_{imp} - Accordingly, the energy capacity of 1 kg mass of tractor and agricultural machine

N_{pow} - The power of the tractor engine is Kw;

k_{pow} - Degree of average engine load;

g_{ind} - Indicative cost of fuel mj/kw.hour

e_{fuel} -Energy capacity 1 kg of fuel, mj/kg;

γ - Specific weight of fuel g/cm^3;

W_{hour} - Hourly production of the aggregate ha/hr, (t.km/hr, t/hr, m^3/hr);

e_{op} - Energy capacity of labor resource, mj/man.hour.

Conclusions:

– There is intellectual property (patent (No. AP 2020 15395).

– Experimental samples have been made.

– Field tests are conducted.

– These aggregates will be tested under different field conditions for different crops.

– The receipt of tributes will be processed and affiliated in local and foreign scientific journals.

– On the basis of the above-mentioned foundations, a project for filing for a scientific grant has been written. For the manufacture of these aggregates in the factory and their implementation and distribution in Georgia.

This article is published using with the support of Shota Rustaveli Georgian National Science Foundation Under the **[Young Scientists Research Grant 2021 - YS-21-342].**

References:

1. **https://www.geostat.ge/ka.**

2. https://www.sakpatenti.gov.ge/ka/search_engine/view/15395/1/. Combined device for the formation of furrows and cover plastic mulch. AP 2020 15395.

3. Giorgi Kutelia, Otar Karchava, Vladimer Miruashvili. Innovativecombined unit for mulching soil on the basis of a Motoblock. International Scientific Conference "Agricultural Mechanization and Technology in Europeand Perspectives", Conference Proceedings. (2022) Pp 123-126.

4. S.I. Chalaganidze a, J.B. Katsitadze b, G.G. Kuteliab,*. The theoretical and experimental study of the ploughs' ploughshares in order to increase the reliability of resource-saving technology using similarity and dimensions theory. Annals of Agrarian Science 15 (2017) Pp.329-331.

5. Otar Karchava. Giorgi Kutelia. Shota Tsukoshvil. Comparative energetically and economic analysis of Intensive farming and Minimum tillage practices of soybean production. Proceedings of IX International Scientific and Practical Conference (2021) Pp 13-17.

Assessment of stability of a forest tractor with a hydraulic arm

Ján Dižo[1,*], Miroslav Blatnický[1], Vadym Ishchuk[1], Denis Molnár[1]
University of Žilina, Faculty of Mechanical Engineering, Žilina, Slovak Republic[1]
jan.dizo@fstroj.uniza.sk

Abstract: *Forests tractors are inseparable part of a forest economy. Forests tractors serve for logging of logs in forests. Current forests tractors are usually equipped by hydraulic arms, which allow to expand the utility of a tractor. A tractor with a hydraulic arm is able to handle with wood logs without a need additional forest machine, which helps to reduce costs. On the other hand, it is necessary to analyse tractors abilities, which has such an additional equipment. This article is focused on assessment of stability of a forest tractor, which is equipped by such a hydraulic arm. It is a newly designed forest tractor which smaller dimensions, which is intended to be used in conditions with requirements for lower contact pressure and better manoeuvrability. As the hydraulic arm changes the centre of gravity of an entire tractor, mainly with the load, safe operation of the tractor needs to know limit conditions of stability under the maximal load and in the given slope inclination.*
Keywords*: STABILITY, SAFETY, TRACTOR, FOREST, HYDRAULIC ARM*

1. Introduction

Consistent technological progress in the field of technics and machine industry has caused significant increase of using special logging tractors (or skidders) for timber harvesting and yarding [1; 2]. Nowadays, yarding by means of logging tractors is the most widely way for timber harvesting in forests not only in Europe, but also around the world [3; 4]. Technologies applied in these special wheeled forest tractors allow to use them in every type of terrain as well as in various gradient of slopes. Recent needs of customers require to design a new and more compact model of a tractor, which would be able to compete other products on the European market.



Fig. 1 *A 3D model of the forest tractor.*

The objective of the presented article is analysis of stability of the tractor, which will serve for logging the wood in forest and which is equipped with a hydraulic arm. The analyzed tractor represents the smallest model of the tractor producer (Fig. 1) and it also represents the logging tractor, which belongs to the smallest tractors in this sector within the European market. The presented solution has arisen due to the need of mounting of a hydraulic arm on the given tractor as a non-standard equipment.

Timber logging can be defined as transposition of logs form a place of harvesting to a place of timber processing or timber transportation. Ground yarding is most often used for slopes up to 40 %, but some logging tractors are able to works on slopes even up to 50 % [1-4].

2. Selection of a hydraulic arm

A winch and a hydraulic arm with a grapple are very important construction units of the solved tractor. The main role of the winch (Fig. 2) is yarding of logs from hardly accessible places nearer to the tractor. The two-drum winch optionally controlled by means of a remote control is mounted on a rear part of a tractor frame and it is included in a base package of the tractor. When logs are near enough to the tractor, an operator can handle the logs by means of the hydraulic arm (Fig. 2). This hydraulic arm will be mounted on the pedestal, which is placed above the winch, whereby operational space of the winch as well as the hydraulic arm must not be limited. Just this component is the objective of the solved task.

Hydraulic arms of logging tractors are mostly placed in a rear part of a tractor frame. Such a conception allows utility of tractors, mainly in a hardly accessible terrain and in bad weather conditions. The solved logging tractor is intended for using in a thinning and premature timber harvesting and for easier yarding of toppled trees and other wood-pulps.



Fig. 2 *A hydraulic arm for the forest tractor*

The hydraulic arm is located on the tractor by means of an adapted pedestal, which is placed above the winch. The hydraulic arm is mounted on the pedestal by ten screws with a cylindrical head and with an internal hexagon. As the hydraulic arm is a nonstandard equipment of the tractor, it is necessary to design such a pedestal structure, which can be installed and removed in a simple way, which will not be time-consuming.

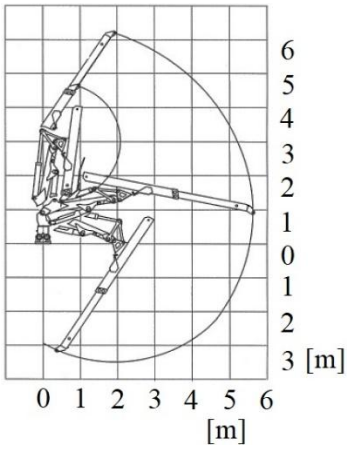


Fig. 1 *Working range of the hydraulic arm.*

In term of a conception, it is a four-wheeled articulated tractor with an all-wheel drive train. A steering system of the tractor contains two hydromotors and vertical pins [5]. Such a system ensures very well manoeuvrability and ability to work in heavy gradient of slopes. The tractor is powered by a four-cylinder four-stroke diesel engine, which is liquid-cooled and turbocharged by a supercharger. The engine meets all valid limits in term of exhaust emissions regulations for ensuring ecological operation [6].

Selection of a hydraulic arm comes out from two terms. On one hand, criterion assessment of various available products has been performed and on the other, requirements of the tractor producer have been taken into account. Fig. 3 shows a working range of the selected hydraulic arm.

3. Stability of the tractor

Work in inaccessible terrains in which tractors work are often affected by dangerous situations when moving these machines. The stability of the machine is a limiting indicator that limits the use of the work machine in dangerous terrains.

Calculation of the center of gravity

To calculate the center of gravity of the hydraulic arm, which is equipped with a grab and rotator without a load, it is necessary to know the x- and y-coordinates of the centers of gravity of all the components that make up the hydromanipulator. In Fig. 4 the coordinates of these components are shown. The blue color shows the position of the center of gravity of the hydraulic arm with its coordinates relative to the coordinate system, which is shown by the yellow *x* and *y* axis. All values of these coordinates are listed in Tab. 1.

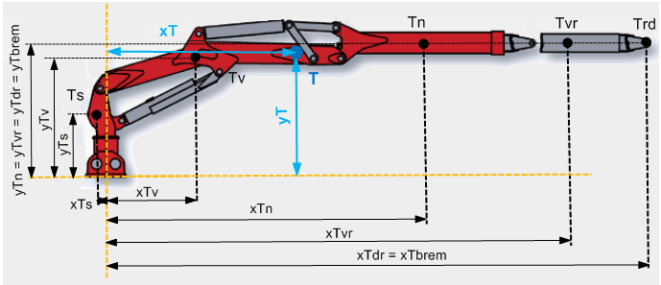


Fig. 4 *Coordinates of individual components of the hydraulic arm.*

Table 1: *Values of coordinates of individual components of the hydraulic arm.*

Centre of gravity	*x*-coordinate	Value [mm]	*y*-coordinate	Value [mm]
T_s	x_{Tv}	30.5	y_{Tv}	460
T_v	x_{Tv}	1189	y_{Tv}	1161.5
T_n	x_{Tn}	3429	y_{Tn}	1403
T_{vr}	x_{Tvr}	5019	y_{Tvr}	1403
T_{dr}	x_{Tdr}	5619	y_{Tdr}	1403

To calculate the *x*-coordinate of the center of gravity x_T of the hydraulic arm, it is necessary to substitute the values into formula (11):

$$x_T = \frac{x_{Ts} \cdot m_s + x_{Tv} \cdot m_v + x_{Tn} \cdot m_n + x_{Tvr} \cdot m_{vr} + x_{Tdr} \cdot m_{dr}}{m_r} \quad (1)$$

where x_{Ti} [mm] are the *x*-coordinates of the centers of gravity of the individual components, m_i [kg] are the weights of the individual components, x_T [mm] is the value of the *x*-coordinate of the center of gravity of the hydraulic arm.

To calculate the *y*-coordinate of the center of gravity y_T of the hydraulic arm, it is necessary to substitute the values into the formula (12):

$$y_T = \frac{y_{Ts} \cdot m_s + y_{Tv} \cdot m_v + y_{Tn} \cdot m_n + y_{Tvr} \cdot m_{vr} + y_{Tdr} \cdot m_{dr}}{m_r} \quad (2)$$

where y_{Ti} [mm] are the *y*-coordinates of the centers of gravity of individual components, m_i [kg] are the weights of individual components, y_T [mm] is the value of the y-coordinate of the center of gravity of the hydraulic arm.

The center of gravity of the hydraulic arm has coordinates *T* [2650; 1150] mm.

Calculation of stability

The calculation of tractor stability depends on the mutual position of the slope of the slope and the tractor. These positions are analyzed in the following chapters also with detailed calculations of the maximum slope angles. To calculate individual stability positions, it is necessary to know the position of the center of gravity of the hydraulic arm, the position of the center of gravity of the load, which is located at the end of the extended arm, the position of the center of gravity of the designed pedestal and the position of the center of gravity of the tractor (Fig. 5). When solving individual stability positions, it is necessary to know the individual loads given in Tab. 2.

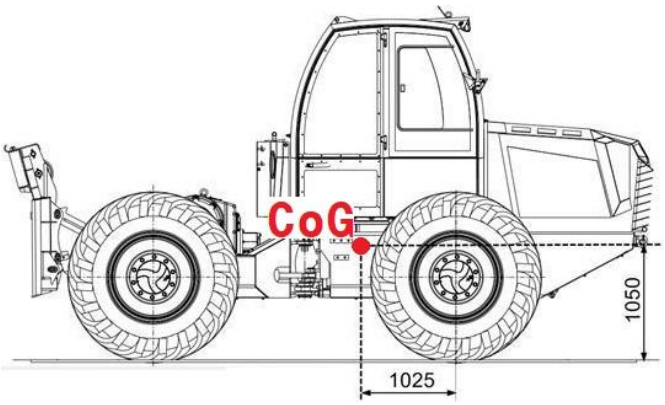


Fig. 5 *The center of gravity of the tractor.*

Table 2: *Values of the loads for the stability analysis.*

	Weight [kg]	Load [N]
Tractor	m_T = 5500	G_T = 53955
Hydraulic arm	m_R = 940	G_R = 9221
Basic plate	m_P = 330	G_P = 3238
Burden	m_B = 850	G_B = 8340
Totally	m_{tot} = 7620	G_{tot} = 15110

When dealing with stability, it is necessary to know that the use of the hydraulic arm while driving the tractor is strictly prohibited. Manipulation with the hydraulic manipulator is only allowed when the tractor is stationary. When solving individual stability positions, it is considered that the tractor is not bent, i.e. the tractor is in a straight position.

The position of the tractor parallel to the contour and the position of the hydraulic arm down the slope

This position (position No. 1) occurs when working in the forest, when the tractor is placed transversely on the slope of the slope and the hydraulic arm is pointing down the slope, with the maximum possible load given by the manufacturer. This situation is depicted in Fig. 6.

The stability solution is performed through the moment equation to point A, while the maximum angle α_1 is investigated, which indicates the limit state when the tractor does not overturn with the hydraulic arm loaded. For the solution, it is necessary to know the distances of the centers of gravity from the pad and the tractor axis, which are calculated in Tab. 3. Although the use of the hydromanipulator is prohibited during driving, an acceleration of

a_{max} = 1.25 m·s^{-2} occurs during a possible start, which causes a dynamic effect. However, in this position, this acceleration does not affect the results achieved.

Table 3: *Values of distances of the center of gravity from the surface and the tractor axis.*

Parameter	Value [m]
x_{max}	5.620
x_R	2.652
L_T	1.250
h_T	1.050
h_P	1.340
h_R	2.490
h_B	2.270

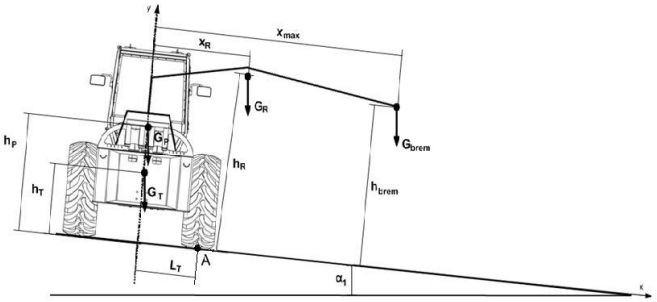


Fig. 6 *Stability position No. 1.*

$$-G_T \cdot \cos\alpha_1 \cdot L_T + G_T \cdot \sin\alpha_1 \cdot h_T - G_P \cdot \cos\alpha_1 \cdot L_T + G_T \cdot \sin\alpha_1 \cdot h_P + G_R \cdot \cos\alpha_1 \cdot (x_R - L_T) + G_R \cdot \sin\alpha_1 \cdot h_R + G_B \cdot \cos\alpha_1 \cdot (x_{max} - L_T) + G_B \cdot \sin\alpha_1 \cdot h_B = 0 \quad (3)$$

$$\cos\alpha_1 \cdot [-G_T \cdot L_T - G_P \cdot L_T + G_R \cdot (x_R - L_T) + G_B \cdot (x_{max} - L_T)] + \sin\alpha_1 \cdot [G_T \cdot h_T + G_P \cdot h_P + G_R \cdot h_R + G_B \cdot h_B] = 0 \quad (4)$$

After substituting the given quantities, the following applies:

$$-22131 \cdot \cos\alpha_1 + 102887 \cdot \sin\alpha_1 = 0$$

$$\tan\alpha_1 = \frac{22131}{102887} \Rightarrow \alpha_1 = 12.15° \quad (5)$$

where α_1 [°] is the limit angle, G_x [N] are the individual loads, h_x [m] are the perpendicular distances of the centers of gravity from the base, L_T [m] is half the length of the width of the tractor.

The resulting limit angle reached the value α_1 = 12.15°, when the tractor is working on a greater slope, the tractor may overturn.

The position of the tractor parallel to the contour and the position of the hydraulic arm on the slope up the slope

This position (position no. 2) occurs when working in the forest, when the tractor is placed transversely on the slope of the slope and the hydraulic arm points up the slope, with the maximum possible load given by the manufacturer. This situation is depicted in Fig. 7.

The stability solution is performed through the moment equation to point A, while the maximum angle α_2 is investigated, which indicates the limit state when the tractor does not overturn with the hydraulic arm loaded. The use of the hydromanipulator itself is prohibited during driving, however, during a possible start-up, an acceleration of a_{max} = 1.25 m·s^{-2} occurs, which causes a dynamic effect. This acceleration does not affect the calculation of stability in position No. 2.

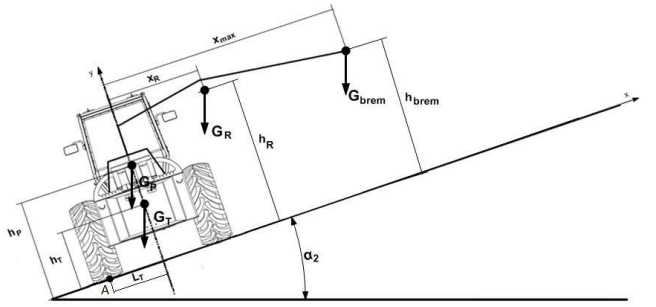


Fig. 7 *Stability position No. 2.*

$$G_T \cdot \cos\alpha_2 \cdot L_T - G_T \cdot \sin\alpha_2 \cdot h_T + G_P \cdot \cos\alpha_2 \cdot L_T - G_T \cdot \sin\alpha_2 \cdot h_P + G_R \cdot \cos\alpha_2 \cdot (x_R + L_T) + G_R \cdot \sin\alpha_2 \cdot h_R + G_B \cdot \cos\alpha_2 \cdot (x_{max} + L_T) - G_B \cdot \sin\alpha_2 \cdot h_B = 0 \quad (6)$$

$$\cos\alpha_2 \cdot [G_T \cdot L_T + G_P \cdot L_T + G_R \cdot (x_R + L_T) + G_B \cdot (x_{max} + L_T)] + \sin\alpha_2 \cdot [-G_T \cdot h_T - G_P \cdot h_P - G_R \cdot h_R - G_B \cdot h_B] = 0 \quad (7)$$

After substituting the given quantities, the following applies:

$$136850 \cdot \cos\alpha_2 - 102887 \cdot \sin\alpha_2 = 0$$

$$\tan\alpha_2 = \frac{136850}{102887} \Rightarrow \alpha_2 = 53.11° \quad (8)$$

where α_2 [°] is the limit angle.

The resulting limit angle reached the value α_2 = 53.11°, when the tractor is working on a greater slope, the tractor may overturn.

Calculation of the axle loads

When solving the load on the individual axles of the tractor, the machine is placed on the plane, while the hydraulic arm is maximally extended and with the maximum possible load. The vertical forces acting on the individual axles must not exceed the maximum permissible static axle load specified by the manufacturer. The following applies to the axles used on the tractor:

- Maximum static load of the front axle F_{PN} = 125 kN,
- Maximum static load of the rear axle F_{ZN} = 125 kN.

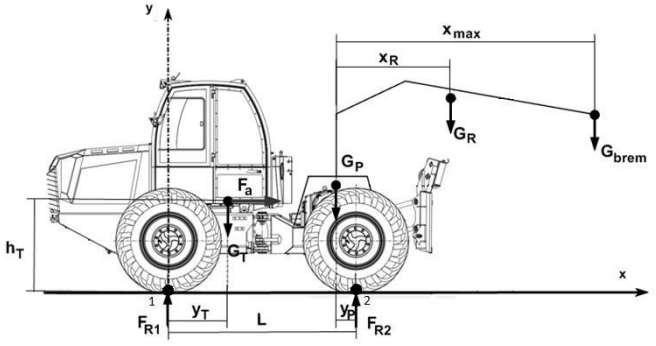


Fig. 8 *The loads on individual axles when the machine is on the straight surface*

Reaction F_{R1} acts on the front axle and reaction F_{R2} on the rear axle. This state is shown in Fig. 8. The use of the hydromanipulator is prohibited during driving, however, during a possible start-up, an acceleration of a_{max} = 1.25 m·s^{-2} may occur, which will cause a dynamic effect. This acceleration causes the inertial force F_a, which is shown in Fig. 8 in gray and is oriented in the opposite direction to the applied acceleration.

The rear axle load given by reaction F_{R2} is given by the moment equation to point 1:

$$G_T \cdot y_T + G_P \cdot (L - y_P) - F_{R2} \cdot L_T + G_R \cdot (L + x_R - y_P) + \\ + G_B \cdot (x_{max} + L_T - y_P) + m_{total} \cdot a_{max} \cdot h_T = 0 \quad (9)$$

$$F_{R2} = \frac{G_T \cdot y_T + G_P \cdot (L - y_P) + G_R \cdot (L + x_R - y_P)}{L} + \\ + \frac{G_B \cdot (L + x_{max} - y_P) + m_{total} \cdot a_{max} \cdot h_T}{L} \quad (10)$$

After substituting the values of forces and distances into equation, we get:

$$F_{R2} = \frac{181225}{2.5} \approx 72490 \text{ N} \quad (11)$$

The front axle load given by reaction F_{R1} is given by the moment equation to point 2:

$$-G_T \cdot (L - y_T) + F_{R1} \cdot L - G_P \cdot y_P + G_R \cdot (-y_T + x_R) + \\ + G_B \cdot (x_{max} - y_P) + m_{total} \cdot a_{max} \cdot h_T = 0 \quad (12)$$

$$F_{R1} = \frac{G_T \cdot (L - y_T) + G_P \cdot y_P - G_R \cdot (x_R - y_P)}{L} + \\ + \frac{-G_B \cdot (x_{max} - y_P) + m_{total} \cdot a_{max} \cdot h_T}{L} \quad (13)$$

After substituting the values of forces and distances into equation, we get:

$$F_{R1} = \frac{25660}{2.5} \approx 10264 \text{ N} \quad (14)$$

The value of the vertical force on the front axle is F_{R1} = 102648 N, which meets the condition set by the manufacturer (F_{PN} = 125 kN). The value of the vertical force on the rear axle is F_{R2} = 72490 N, which also meets the condition set by the manufacturer (F_{ZN} = 125 kN).

4. Conclusion

The objective of this contribution was to analyses the stability conditions of the forests tractor. The analyses come from the determination of the center of gravity position. Subsequently, two positions of the tractor on a slope were analyzed. The calculations shown, that the tractor has better stability for the position No. 2. This fact is given, that in the position No. 1, the transported wood logs lead to greater moment, which overturn the tractor. IN the position No. 2, the wood logs lead to stability moment. Finally, the loads of the both axles were calculated. The analysis shown, that the rear axle is more loaded than the front axle. This is caused by the fact, that the wood logs are transported in the rear part of the tractor. Therefore, the load is greater on the rear axle.

5. Acknowledgements

This contribution was supported by the project KEGA 031ŽU-4/2023: Development of key competencies of the graduate of the study program Vehicles and Engines.

This contribution was supported by the project KEGA 036ŽU-4/2021: Implementation of modern methods of computer and experimental analysis of the properties of vehicle components in the education of future vehicle designers.

6. References

1. J. Kašpárek, M. Skopán, M. Sedláček, Proceedings of the 22nd International Scientific on Conference "Transport Means 2018", 2018, Trasalis-Trakai, Lithuania, 2018, pp. 537-541.
2. J. Kašpárek, M. Škopán, M. Jonák, P. Pokorný, Proceedings of the 20th International Scientific on Conference "Transport Means 2016", 2016, Juodkrante, Lithuania, pp. 751-755.
3. I. Shegelman, P. Budnik, V. Baklagin, Croatian J. of For. Eng. **40**, 297-310 (2019)
4. M. Nikooy, S. Ahrari, A. Saleri, R. Naghdi, J. of For. Science **61**, 393-398 (2015)
5. Ch. Yin, Q. Sun, J. Wu, Ch. Liu, J. Gao, J. of Electrical and Comput. Eng. **2018**, 1-7 (2018)
6. J. Wasilewski, A. Kuranc, J. Szyszlak-Barglowicz, M. Stoma, T. Slowik, D. Barta, Proceedings of IX International Scientific Symposium "Farm Machinery and Processes Management in Sustainable Agriculture", 2017, Lublin, Poland, 2017, pp. 406-410.

Experimental study of the driving resistance of a harrow with screw working bodies

Volodymyr Bulgakov[1]; Ivan Holovach[1]; Mykola Klendii[2]; Oleksandra Trokhaniak[1]; Yevhen Ihnatiev[3]; Olha Dubrovina[1]

[1]National University of Life and Environmental Sciences of Ukraine, Kyiv, Ukraine
[2]Separated Subdivision of National University of Life and Environmental Sciences of Ukraine
Berezhany Agrotechnical Institute, Berezhany, Ukraine;
[3]Dmytro Motornyi Tavria State Agrotechnological University, Ukraine
E-mail: vbulgakov@meta.ua

Abstract. *The article presents the construction and manufacturing of working screw harrow bodies, as well as the developed experimental setup for experimental studies, presents the methodology of research to determine the traction resistance of the working body. The variations of traction resistance force P_x from the speed of harrow movement V, at different values of the angle of attack β of working screw bodies and working depth h are plotted.*
KEYWORDS*: HARROW WITH HELICAL WORKING TOOLS, HARROW SPEED, WORKING DEPTH, TRACTION.*

1. Introduction

Soil-cultivating working tools of agricultural machinery create the necessary conditions for intensive growth and development of plants: the access of oxygen and moisture to the soil is facilitated, the root system develops faster, the plant intensively absorbs macro- and microelements from the soil and, as a result, the potential of biological yields increases.

To reduce the cost of technological operations while maintaining the productivity of agricultural machinery and the quality of their performance, it is necessary to create new agricultural machinery, their working bodies and conduct appropriate research and develop recommendations for the effective cultivation of crop production.

The main trend in the development of means of mechanization of basic soil cultivation is their rational differentiation. Technologies, units and complexes for tillage are being improved in the direction of ensuring the quality of tillage and reducing energy consumption. Attempts to reduce traction and specific resistance of agricultural machines require continuous research of more perfect, in terms of energy intensity, working tools and technologies of field works.

Traction resistance is a value that constantly changes during operation. All factors affecting the traction resistance of the machine can be classified as follows: natural and climatic (type and condition of the ground, topography, stoniness, meteorological conditions); constructive (type, shape and number of working tools, the material from which they are made and manufacturing technology, machine weight, type and construction of the chassis); operational (technical condition of the machine, the accuracy of adjustment, degree of wear of working tools, etc.) [1-3]. In works [4, 5] theoretically justified design of tillage implements, in which, as working elements are used helical surfaces from the compartment of helicoid.

The definition and solution of the problem of selecting the optimal parameters of the helical working body of tillage machines with the condition of minimizing their material intensity [6] and energy consumption [7] are known.

The purpose of the work is to determine the traction resistance of a harrow with helical working tools, depending on the change in the angle of attack of the working tool, the depth of tillage and the speed of the harrow.

2. Materials and Methods

To conduct experimental research on the basis of theoretically obtained construction parameters of helicoid coils, the construction was developed and manufactured working tools of the harrow, the construction of which is shown in Fig. 1. To avoid blocking the space between the coils with soil, it is proposed to make the cylindrical shaft with a lattice.

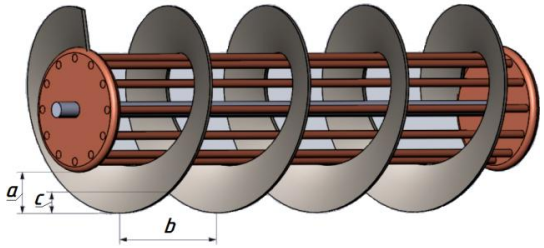


Figure 1*. Screw tillage tool with a sieve shaft: a – working depth, c – ridge height, b – distance between ridges*

The body operates similar to disk implements, that is, the profile of the cultivated field has ridges and troughs. At the moment of contact of the blade with the field surface, there are angles similar to the angles of attack and roll for disk implements. The roll angle can be changed by changing the inclination of the rectilinear forming surface with respect to its axis.

The developed tool has a simple construction and low metal consumption. In contrast to disk implements, it does not require individual bearing assemblies for mounting individual tillage discs. One section of the helical tillage tool is mounted by means of two bearing assemblies on the ends of the section.

As a result of the interaction of the working body with the soil, a reaction force arises, which will press on the working surface of the coil. The component of this force will try to move the implement perpendicular to the direction of its movement. In order to balance this moment of force, it is advisable to arrange the unit as two implements, as shown in Fig. 2.



Figure 2*. General view of harrow with screw working tools*

The surface of the second implement should have a turn-over rib with the opposite direction of the winding and the direction of the straight formations. The cylindrical shaft for the implement has been selected for a given depth and cultivation. Also with this variant it is possible to reduce the height of ridges *c* and distance *b* between ridges.

Table 1 shows the technical characteristics of the harrow with screw working tools.

Table 1 *– Technical characteristics of the harrow with screw working tools*

Parameter	Values
Structural working width, m	1.3
Required tractor power, kW	от 18
Coupling with a tractor	mounted
Mass, kg	172
Number of helicoid turns, pcs.	10
Outer diameter of the screw, mm	562…570
Processing depth, cm	6…10
Operating speed, km·h^{-1}	7...17
Overall dimensions in transport position, mm	2090×1430×1250

To determine the traction resistance of the proposed harrow with screw working tools, an experimental setup was used, the general view of which is shown in Fig. 3.

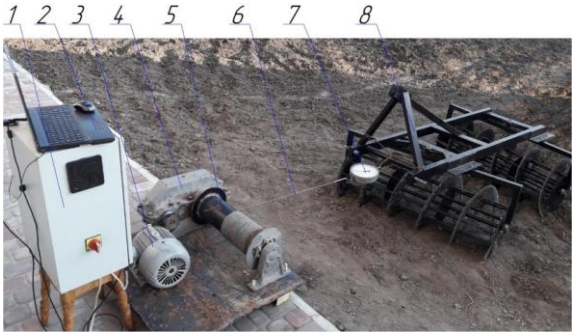


Figure 3*. Experimental setup for determining the traction resistance of a screw with screwed working tools*

The harrow with the screw working bodies 8 was driven by the cable 6, which in the process of movement was wound on the drum 5, fixed on the slow-speed shaft of the reducer 4, driven by the electric motor 3. The Altivar 71 frequency converter (1) and the Power Suite v.2.5.0 software contained in the PC (2) were used for starting the motor and regulating its rotation frequency. The electric motor 3 and gearbox 4 were rigidly fixed at the beginning of the soil channel to be stationary, and only the harrow was movable.

Determination of traction resistance offered by the harrow with helical working tools was carried out in the soil channel with dimensions 3.5×30 m (the length of the control section is equal to 25 m).

The values of torque and engine power were fixed as a percentage of the nominal value. The motor power was determined from the product of the rated motor power by the maximum percentage value of the selected mode.

It should also be noted that the torque by the inverter is calculated by a mathematical model and the error can reach 20% (or 5% in the mode with encoder feedback).

Experiment scheme: performance of technological process by the unit for the purpose of surface loosening of the soil, closing moisture, seeding, destruction of weeds, as well as for leveling the micro-relief created by pre-treatment. The number of repetitions – three.

In the experimental studies, we used a planar method, which provides determination of the resultant force acting between the electric motor with gearbox and harrow, in one plane (longitudinal-vertical).

Before each stage of the experiment, the harrow with a screw working body was located in the extreme right position, the soil in the channel was previously prepared according to the hardness meter readings.

The results of investigations in the soil channel of the proposed harrow with a screw implement were illuminated in the computer display window.

Then, according to the peak values, the obtained results were recorded in tables. Experiments were conducted for four harrow movement speeds, namely: V = 4.0; 6.0; 8.0 and 10.0 kg·h^{-1}. To change the speed of harrow moving, the frequency of voltage supplied to the motor was changed with the help of frequency converter.

3. Results and discussions

According to the results of the obtained researches the graphical dependencies of traction resistance P_x on the harrow movement speed V, at different values of the attack angle β of screw working tools and tillage depth h were plotted.

Fig. 4 shows the graphical dependences of traction resistance P_x of the proposed harrow with helical working tools with the attack angle β = 30° on the movement speed V at different working depths h = 0.06 – 0.10 m.

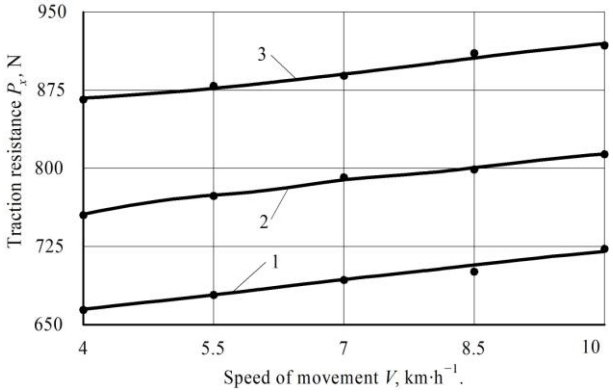


Figure 4*. Plots of traction resistance P_x of the proposed harrow with helical tools with angle of attack β=30° on the movement speed V at the working depth:*
1 – h = 0.06 m; 2 – h = 0.08 m; 3 – h = 0.10 m

According to the results of the analysis of graphs (Fig. 4) it is established that the traction resistance P_x of the offered harrow with the screw tools at working depths from h = 0.06 m to the maximum h = 0.10 m at the set angle of attack β = 30° grows linearly from 665 N to 716 N at h = 0.06 m, from 762 N to 812 N at h = 0.08 m; and from 874 N to 924 N at working depth h = 0.10 m. The analysis of graphic dependencies shows, that with the increase of traction speed of the harrow with screw working tools V from 4 to 10 km·h^{-1}, traction resistance P_x grows, and for the depth h = 0.06 m, P_x grows by 7.1%, for h = 0.08 m – by 6.2% and for the depth of cultivation h = 0.10 m, P_x grows by 5.4%. It can also be noted that increasing the processing depth with h = 0.06 m to h = 0.10 m at the speed of the harrow V = 4 km·h^{-1} leads to an increase in traction resistance by 22.5%, and at V = 10 km·h^{-1} resistance increases by 23.9%.

Fig. 5 shows the graphical dependencies of traction resistance P_x of the proposed harrow with screw tools for the movement speed V = 8 km·h^{-1} from the angle of attack β, at different working depths h = 0.06 – 0.10 m.

Analysis of the graphical dependencies (Fig. 5) shows that for the suggested harrow with helical tools at travel speed V = 8 km·h^{-1} for working depths h = 0.06 m, h = 0.08 m and h = 0.10 m the traction resistance within the limits of the attack angle β = 20°...30° grows slowly, and with further increase of the attack angle β, the traction resistance grows more intensively and at β = 40° reaches the values P_x = 891 N at the nominal working depth h = 0.06 m, P_x =1018 N at the working depth h = 0.08 m and P_x =1182 N at the maximum working depth h = 0.10 m. Slow change of traction resistance within β = 20°...30° occurs because due to geometrical features of working surface of working body the contact area of helical spiral surface with soil grows.

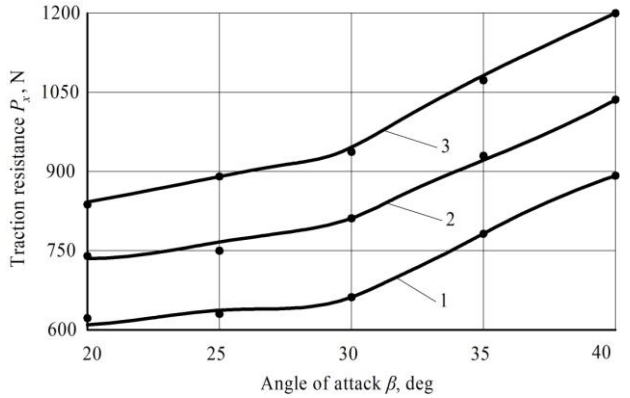


***Figure 5**. Plots of traction resistance P_x of proposed harrow with screw working tools for the movement speed V = 8 km·h^{-1} from the angle of attack β at the working depth: 1 – h = 0.06 m; 2 – h = 0.08 m; 3 – h = 0.10 m*

Also it may be noted, that the increase of tillage depth from h = 0.06 m to h = 0.10 m, with the attack angle of screw working tools β = 20°, leads to increase of traction resistance by 25.1 %, at β = 30° the traction resistance increases by 27.5 %, and with β = 40° the traction resistance increases by 24.6 %.

Fig. 6 shows the graphical dependences of traction resistance P_x of the proposed harrow with helical working tools with angle of attack β = 30° on the depth of soil cultivation h at different speeds of harrow movement V = 6–10 km·h^{-1}.

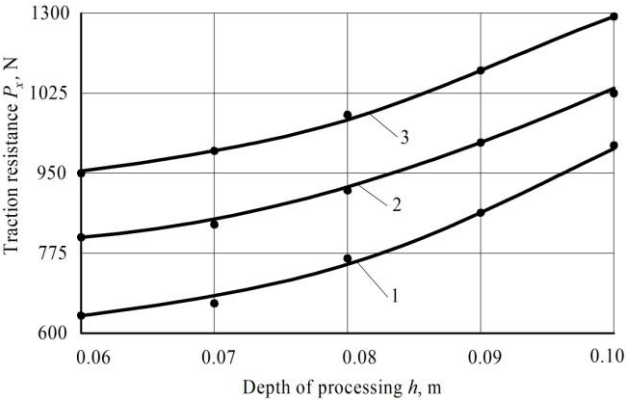


***Figure 6**. Plots of traction resistance P_x of the proposed harrow with helical tools with angle of attack β=30° as a function of working depth h at moving speed: 1 – V= 6 km·h^{-1}; 2 – V = 8 km·h^{-1}; 3 – V = 10 km·h^{-1}*

According to the results of analysis of dependencies (Fig.6) It is established that the traction resistance P_x, the suggested harrow with helical cutting tools at travel speeds from V = 6 km·h^{-1} to maximum V = 10 km·h^{-1}, at set cutting tool angle β = 30° increases curvilinearly from 648 N to 968 N at V = 6 km·h^{-1}, from 823 N to 1109 N at V = 8 km·h^{-1}; and from 978 N to 1279 N at harrow travel speed V = 10 km·h^{-1}.

The analysis of the graphical dependencies shows that with the increase of tillage depth h from 0.06 m to 0.10 m the traction resistance P_x increases, whereas for the harrow's speed V = 6 km·h^{-1} P_x increases by 16.3 %, for V = 8 km·h^{-1} by 12.5 % and at the harrow speed V = 10 km·h^{-1} P_x increases by 14.4 %. According to the recommendations for two track harrows depending on the soil properties, working depth and the angle of attack the resistivity is k = 1500...3000 N·m. Thus, for a standard disc harrow with the working width B = 1.3 m the value of the traction resistance under the most favorable parameters is approximately 2000 N. This value of the traction resistance is significantly greater (approximately 1.3 times) than the values of traction resistance obtained during experimental researches of the offered harrow with helical working elements. Such decrease of the traction resistance can be explained by the absence of the back angle of a working surface in the form of a unfolding helicoid, at optimum values of the attack angle β = 20° – 40° and nominal working depth h = 0.10 m.

4. Conclusion

There are presented the construction and manufactured working screw working bodies of the harrow, as well as the developed experimental setup for experimental studies, presented the methodology of research to determine the traction resistance of the working body. The results of experimental studies of determining the traction resistance of the harrow with helical working bodies are presented. According to the results of the experimental studies the graphical dependences of changes in the angle of attack of the working body, the depth of tillage and the speed of the harrow are plotted.

On the basis of the research it was found that an increase in working depth from h = 0.06 m to h = 0.10 m, resulted in an increase of traction resistance by 22.5 – 23.9 %, an increase in harrow speed from V = 6 km·h^{-1} to V = 10 km·h^{-1}, resulted in an average increase in traction resistance by 14.5 % and increase of screw working body attack angle up to β = 20° leads to the increase of traction resistance by 25.1 %, at β = 30° traction resistance is increased by 27.5%, and with β = 40° traction resistance is increased by 24.6%.

5. References

1. Klendii, M.B., Pilipaka, S.F.Analytical model of installation of tillage spherical disks for determination of geometric and technological characteristics - Scientific Bulletin of the National University of Life and Environmental Sciences of Ukraine, issue 241, 2016, pp. 140-150.

2. Bulgakov, V., Pilipaka, S., Adamchuk, V. Olt, J. Theory of motion of a material point along a plane curve with a constant pressure and velocity. – Agronomy Research, Estonian Agricultural University, vol. 12(3), 2014, pp. 937-948.

3. Pilipaka, S.F., Babka, V.N., Zaharova, T.N. Forma osi gibkoy neszhimaemoy polosi pri ee tolkanii po naklonnoy sherohovatoy ploskosti s postoyannoy skorostyu, Motrol, vol. 15, no. 4, 2013, pp. 198-205.

4. Lech M. Mass flow rate measurement in vertical pneumatic conveying of solid. – Powder Technology, vol.114, Issues 1–3, 2001, pp. 55-58.

5. Bulgakov V., Olt J., Ivanovs S., Trokhaniak O., Gadzalo Ja., Adamchuk V., Chernovol M., Pascuzzi S., Santoro F., Arak M. Research of a contact stresses in swivel elements of flexible shaft in screw conveyor for transportation of agricultural materials. – Estonian Academic Agricultural Society. Agraarteadus, vol. 33, no. 1, 2022, pp. 67-73. doi:10.15159/jas.22.12.

6. Hevko R. B., Rozum R. I., Klendiy O. M. Development of design and investigation of operation processes of loading pipes of screw conveyors. – INMATEH: Agricultural engineering, vol.50, no.3, 2016, pp.89-94.

7. Pylypaka, S., Klendii, M., Klendii, O. Particle motion on the surface of a concave soil-tilling disk. ACTA POLYTECHNICA, Journal of Advanced Engineering, is a peer-reviewed, vol. 28 Issue 3, 2018, pp. 63-73.

Design and strength analysis of the end carriage beam for the single girder bridge crane of a 500 kg load capacity

Denis Molnár[1,*], Miroslav Blatnický[1], Dalibor Barta[1], Juraj Grenčík[1]
University of Žilina, Slovakia[1]
denis.molnar@fstroj.uniza.sk, miroslav.blatnicky@fstroj.uniza.sk, dalibor.barta@fstroj.uniza.sk, juraj.grencik@fstroj.uniza.sk

Abstract: *Overhead cranes are used in production halls, industrial buildings, transshipment yards, automobile factories, as well as in agricultural warehouses. The end carriage is an essential part of any overhead crane. Special attention is focused on the end carriage beam, which is a fundamental component of the end carriage in terms of load and strength. The introductory part of the paper aims to introduce the crane issues, particularly with respect to bridge cranes. The paper attends to the design of the end carriage beam for a single girder bridge crane with a 500 kg load carrying capacity including a strength analysis of the proposed beam. On the basis of the input load data of the end carriage beam and dimensions of area on which the main girder is placed on the end carriage beam, the minimum section modulus in bending was determined through the Allowable Stress Method as a critical parameter for the selection of the end carriage beam. The calculated value of the minimum section modulus in bending is 1416.18 mm^3, based on which the U4O beam profile of S235 JR material was selected. One of the objectives is to create a 3D CAD model of the proposed end carriage beam and subsequently perform FEM analysis of the beam using Ansys engineering simulation software. The purpose of the analysis is to determine the maximum bending stress and maximum deflection of the end carriage beam. The results of the FEA analysis demonstrate that the proposed beam is satisfactory in terms of allowable stress and deflection. Moreover, the beam designed in this manner along with the numerical simulation results provides a precondition of its possible future production.*

Keywords*: END CARRIAGE, BEAM, STRENGTH ANALYSIS, BRIDGE CRANE, DESIGN*

1. Introduction

The transportation and handling of materials from one place to another is one of the basic activities in all manufacturing industries. This activity is performed and ensured by means of transport and handling technology, which is a special field in terms of engineering production. A relatively wide spectrum of machines and equipment represent load lifting equipment, which chiefly includes cranes [1,2]. Since its invention, the crane has been utilized as an important part of the work environment. They are frequently employed in lifting heavy loads as well as in the construction industry. Different types of cranes are available for different requirements. Each type of crane is produced in order to meet the specific requirements of the users [3]. Thus, cranes are pieces of machinery used to move loads, lifting, travelling, turning or changing the position of crane boom, commonly by combining several movements [4]. Cranes can be classified from several points of view, as follows:

- In terms of motion – fixed cranes, mobile cranes, crawler cranes, floating cranes, and others,
- In terms of a type of the drive – manual, electric, hydraulic, combined and others,
- According to external shape of steel structure – bridge cranes, overhead cranes, gantry, semi-gantry cranes, jib cranes, vehicle-mounted cranes, tower cranes, and others,
- According to the operating place – workshop cranes, tower and mobile construction cranes, railroad cranes, harbor cranes, metallurgical cranes, and others.

In addition, from the point of view of the type of operation (rate of loading), cranes are divided into 5 fundamental groups denoted with Roman numerals:

0. – for very light operation (maintenance and repair cranes),
I. – for light operation (assembly and repair cranes),
II. – for medium operation (workshop, construction cranes),
III. – for heavy operation (workshop, foundry, casting, grab cranes),
IV. – for very heavy operation (tongs, forging, casting cranes) [5].

Bridge cranes belong to the most widely employed cranes. This type of cranes ensures the movement of material commonly over a rectangular area designed for material handling. They are one of the chief devices for handling and lifting in factories, warehouses and transshipment yards. Thus, overhead cranes are widely utilized in various fields, such as heavy industries, seaports, automobile factories and construction facilities as well as special buildings, for instance, reactor buildings and turbine buildings [1,6].

2. Bridge cranes

The overhead crane can be denoted as a machine that is capable of lifting and lowering heavy objects and moving them from one place to another. In other words, overhead cranes are complex crane machines designed to carry loads in the horizontal and vertical planes. In terms of design, they represent cranes with one or two main girders depending on the size and load range [7]. Generally, overhead crane is based on three separate movements:

1. The first movement is represented by the hoist, whose function is to raise and lower the material.
2. The second motion is ensured by the trolley (cross travel), which allows the hoist to be positioned directly above the material.
3. The third is the movement of the gantry or bridge (long travel), which allows the motion of the entire crane along its operating area.

The design of bridge cranes varies greatly according to their main operating specifications. These specifications can comprise the type of movement of the crane structure, the mass and type of load, the location of the crane, the geometric characteristics, the operating modes and the environmental conditions [1,2].

In terms of designing the bridge crane, it is required to focus on sizing of appropriate cross-sections and concentrate on the calculation of overall strength of the crane from the point of view of safe operation. Moreover, it is necessary to select the most suitable and relatively reliable structural solution. The following features are crucial in terms of the design and construction of overhead cranes: functionality, operational safety, technical protection, low costs, uncomplicated replacement of damaged parts, aesthetic shape, simple inspection and handling, utilization of simpler technologies in fabrication and assembly [1,2,7]. Inasmuch as the crane structure is affected by load carrying capacity, fatigue loading, material aging and overloading during operation, the critical metal structure of the overhead crane such as the center of span of the main girder, the web of the end girder, the bolted connection and the heat affected welding zone [2, 3] will cause inevitable accumulation of damage. Therefore, it is indispensable to scrutinize the stress state in the precarious position of the metal structure of the crane [8].

A crane cat (or trolley) moves along the rails on the main girders of the bridge (Fig. 1). Single girder bridge cranes are designed in order to cover a wide range of requirements of modern industry. The obvious advantage for this solution is the high added value of the investment without compromising on performance. The single girder bridge crane has a lower weight or vertical wheel load due to its optimized design, which is reflected in cost savings for building state-of-the-art support structures as well as in increased

load capacity of existing structures. Different types of crane girders and lifting device locations can be employed in the design in order to ensure optimum utilization of the available travelling space. Accordingly, the space requirements of the crane can be reduced by up to 50 %. Different types of rope and chain hoists moving along the bottom edge/beam flange are employed as standard equipment due to their low demand on the dimension of the top space. When systems with larger lifting capacities of 10 tons or more are required, it is generally preferable to consider the use of a double girder bridge crane for the sake of the optimization of dimensions and performance. This type of cranes can lift, transport and place almost anything precisely to its location anywhere in crane working area [9,10].

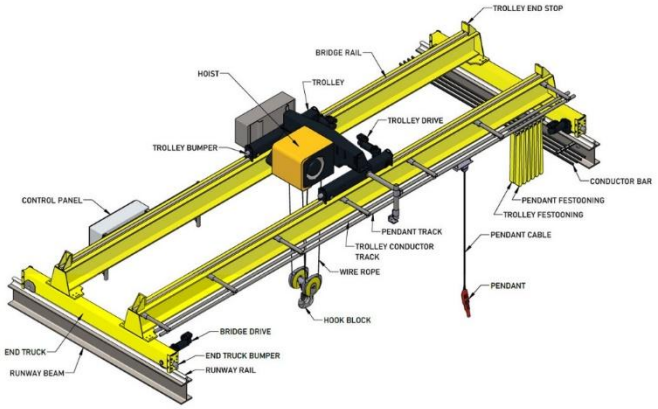


Fig. 1 *A double girder bridge crane and its components* [17].

The selection of the proper type of bridge crane is essential for streamlining workflow and maximizing productivity. Many factors are considered in the process of selection, for example, the required length of the runway, the operating time of crane, the lift height demand, whether the bridge crane will be fixed against the walls of the building or will be of a separate design, and others [11-13].

3. End truck of a bridge crane

The end trucks are an integral part of the entire structure of the double girder bridge crane and symbolize extremely responsible part of the crane. The end truck is positioned on both sides of the bridge and is equipped with wheels on which the entire crane moves. In addition to ensuring the motion of the whole bridge crane structure along the crane runway, it is necessary to meet the conditions of strength, rigidity, and stability. All loads are transferred from the main girders to the crane runway by means of the end trucks. Some of these loads depend on the design of the entire overhead crane structure, the type of trolley and the movement conditions. For the sake of these reasons, special scrutiny should be subjected to design of the end trucks [14].

For the sake of bridge crane manipulation along the crane runway (translational motion) in terms of the performance of the desired functions, a suitable drive for this movement is required, as well as the type of construction. For this reason, end trucks are employed, which along with the main girder form the steel structure of the overhead crane. The principal function of the end truck is to move the entire structure of the overhead crane along the crane runway in addition to ensuring the stability and rigidity of the entire structure of the overhead crane. For these reasons, the end trucks are responsible parts in the whole structure of the overhead crane, thus the selection of the geometrical characteristics of the cross-sections of these girders is crucial. Generally, box sections (both standard and welded, depending on the load capacity) are most utilized elements for the construction of end trucks. Nevertheless, other forms of sections are employed [15,16].



Fig. 2 *Construction of the end truck and its components* [18].

Bridge crane end trucks are the long traveling mechanism of overhead cranes and gantry cranes. The end truck (Fig. 2) is made up of various structural elements, for instance, end truck beam, end truck motor, wheels, bearings, axles, overhead crane brake mechanism, overhead crane gearbox, end truck bumper [11].

End trucks is commonly motorized and have at least 4 forged steel wheels equipped with sealed tapered roller bearings. End trucks shall be produced as one-piece welded structure and designed in order to distribute the weight of the crane and its load evenly between the wheels. They shall be equipped with appropriate drop stops that prevent the crane from falling further than 25 mm in case of breakage of an end truck wheel, bogie or axle. Moreover, end trucks shall be designed to engage into the side of the rail in case of a guide roller collapse and stop the crane safely [1].

4. Design of an end truck beam

The proposed end truck beam is a component of the designed single-girder bridge crane with a load capacity of 500 kg, which is depicted in Fig. 3. For the stated bridge crane, the main girder has already been designed and checked by means of the strength analysis. The main girder and results of analysis are stated in the paper [19]. Moreover, the crane hook was designed for the single girder bridge crane and is addressed by the authors in the paper [20]. Furthermore, the design of the steel rope was carried out for this bridge crane, as well as the design and strength analysis of the rope drum that the authors discuss in detail in the paper [21].

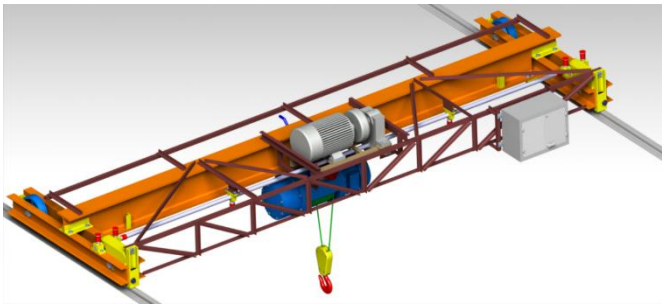


Fig. 3 *Designed single girder bridge crane with a 500 kg load capacity* [19].

4.1 Determination of the end truck beam load

In recent years, efforts to achieve greater efficiency in the use of materials have led to lighter and more flexible lifting machine designs. Increasing operating speeds of modern lifting machines have resulted in enhancing dynamic loads. In terms of engineering practice, dynamic coefficients stated in STN 27 0103 are employed in strength calculations in order to take account the dynamic effects. The values of the coefficients are assigned to the individual crane groups. The groups are formed based on the rate of loading and the magnitude of operating speeds. Statically acting quantities are multiplied by these coefficients (for example, static forces, bending moments, shear forces). Thus, the actual loading effects will be larger by certain dynamic components [2,13]. Therefore, the values of the individual loads are increased by the dynamic coefficients determined according to STN 27 0103 standard in the presented

case [22]. For the factor considering the self-weights, value γ_g = 1.1 (-) is chosen, and for the factor considering the weight of the load, the value γ_{lo} = 1.3 (-) is selected.

The end truck beam is affected by the weight of the main beam and the weight of all the components attached to it. This influence is manifested through the distributed load acting on the end truck beam in its center (see Fig. 4.).

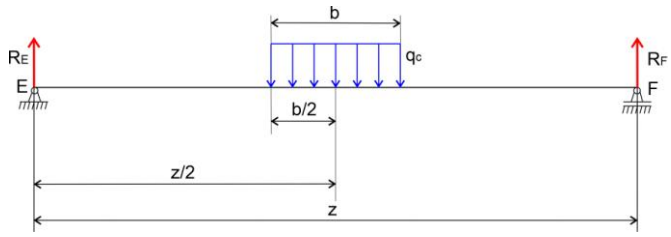


Fig. 4 *The load acting on the end truck beam.*

For the sake of determination the value of the distributed load q_c, it can be employed the equation (1). The magnitude of the load is considered to be a quarter, since there are two beams of one end truck (Fig. 3).

$$q_c = \frac{(m'_N + m'_M + m'_B) \cdot g}{4 \cdot b}, \tag{1}$$

kde b – width of the main girder, m'_N – mass of the main girder of the crane bridge increased by a coefficient γ_g (2):

$$m'_N = m_N \cdot \gamma_g ,$$
$$m'_N = 12.333 \cdot 1.1 = 13.57 \text{ kg}, \tag{2}$$

further m'_M – mass of the crane cat m_M increased by the coefficient γ_g and mass of the hook block m_{kl} increased by the coefficient γ_{lo} (3):

$$m'_M = m_M \cdot \gamma_g + m_{kl} \cdot \gamma_{lo} ,$$
$$m'_M = 32.4 \cdot 1.1 + 3 \cdot 1.3 = 39.54 \text{ kg}, \tag{3}$$

ultimately, m'_B – mass of the load m_B increased by the coefficient γ_{lo} (4):

$$m'_B = m_B \cdot \gamma_{lo} ,$$
$$m'_B = 500 \cdot 1.3 = 650 \text{ kg}. \tag{4}$$

After determining the necessary quantities, it is possible to calculate the distributed load according to equation (1):

$$q_c = \frac{(13.57 + 39.54 + 650) \cdot 9.81}{4 \cdot 55} = 31.352 \text{ N} \cdot \text{mm}^{-1}, \tag{5}$$

4.2 Sizing of the end truck beam

The Allowable Stress Method is used for sizing, which states that the stresses arising in all cross-sections σ_{max} must be less than the given allowable stress σ_{dov} (6).

$$\sigma_{max} \leq \sigma_{dov} . \tag{6}$$

In order to determine the value of the maximum allowable stress, formula (7) is employed, where the safety value k is chosen as k = 1.6 (-). The material of the proposed beam is S235JR steel with a yield strength value of R_e = 235 MPa, which is utilized for end truck beams.

$$\sigma_{dov} = \frac{R_e}{k},$$
$$\sigma_{dov} = \frac{235}{1.6} = 146.875 \text{ MPa}. \tag{7}$$

Due to selection of a suitable cross-section of the beam, it is necessary to calculate the minimum value of the section modulus $W_{o\,min}$. The equation (8) applies to σ_{max}:

$$\sigma_{max} = \frac{M_{Mmax}}{W_{omin}}. \tag{8}$$

After substituting (6) into formula (8) and its subsequent adjustment, the relation (9) for calculating the minimum value of the section modulus in bending $W_{o\,min}$ is obtained:

$$W_{omin} = \frac{M_{Mmax}}{\sigma_{dov}}. \tag{9}$$

Fig. 4 clearly demonstrates that the maximum bending moment MMmax occurs in the center of the beam. The maximum bending moment that occurs in section II (Fig. 5) is determined.

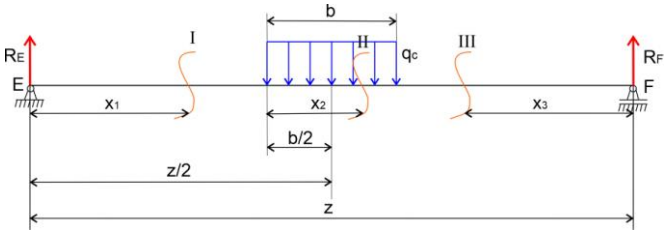


Fig. 5 *Sections of imaginary cuts on the beam.*

In section II, the bending moment M_{o2} is calculated according to the following formula (10):

$$M_{o2} = \frac{q_c \cdot b}{2} \cdot \left(\frac{z}{2} - \frac{b}{2} + x_2\right) - q_c \cdot \frac{{x_2}^2}{2}. \tag{10}$$

where q_c – distributed load acting on the beam, b – width of the main girder of the bridge crane [19], z – length of the end truck beam, x_2 – the distance of the section II from the beginning of the distributed load.

The maximum bending moment occurs in the middle of the beam (Fig. 5), therefore (11) is applied:

$$x_2 = \frac{b}{2}. \tag{11}$$

In addition, equation (12) holds for this case:

$$M_{o2} = M_{Mmax} . \tag{12}$$

After substituting (11) and (12) to formula (10), the equation (13) is obtained:

$$M_{Mmax} = \frac{q_c \cdot b}{2}\left(\frac{z}{2} - \frac{b}{2} + \frac{b}{2}\right) - q_c \cdot \frac{\left(\frac{b}{2}\right)^2}{2}. \tag{13}$$

The equation (14) is provided by means of subsequent adjustment:

$$M_{Mmax} = \frac{q_c \cdot b \cdot (2 \cdot z - b)}{8}. \tag{14}$$

After substituting the values, the value of the maximum bending moment M_{Mmax} is obtained (15):

$$M_{Mmax} = \frac{31.352 \cdot 55 \cdot (2 \cdot 510 - 55)}{8} = 208001 \text{ N} \cdot \text{mm} \tag{15}$$

The end truck will consist of two U profiles (two end trucks, thus, totally 4 beams). After substituting the values, the minimum section modulus W_{omin} for the end truck beam according to formula (9) is determined:

$$W_{omin} = \frac{208001}{146.875} = 1416.18 \text{ mm}^3 . \quad (16)$$

4.3 A selection of the end truck beam

When choosing a beam, condition (17) must be met:

$$W_o \geq W_{omin} , \quad (17)$$

where W_o – section modulus of the proposed end truck beam, W_{omin} – minimal section modulus.

The selection of the suitable beam is based on the calculated value of the minimum section modulus (16). The hot-rolled U40 profile made of material S235JR / 1.0038 from the Ferona catalog [23] is selected for the end truck. Fig. 6 shows the selected beam profile.

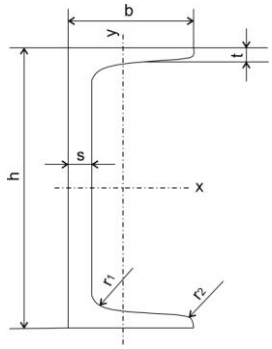


Fig. 6 *Cross section of the U40 profile.*

The parameters of the selected U40 beam section is stated in Table 1.

Table 1 *Parameters of proposed beam U40* [23].

Parameter	Notation	Value	Unit
Height of the profile	h	40	mm
Profile width	b	35	mm
Web thickness	s	5	mm
Flange thickness	t	7	mm
Cross-sectional area	A	621	mm^2
Mass per unit length	m_l	4.87	$kg.m^{-1}$
Radius of inner fillet	r_1	7	mm
Radius of flange fillet	r_2	3.5	mm
Moment of inertia about the x-axis	I_x	14.1	cm^4
Moment of inertia about the y-axis	I_y	6.68	cm^4
Section modulus to the x-axis	W_{ox}	7050	mm^3
Section modulus to the y-axis	W_{oy}	3100	mm^3
Radius of inertia to the x-axis	i_x	15	mm
Radius of inertia to the y-axis	i_y	10.4	mm

5. 3D model and FEM analysis of the end truck beam

Finite element analysis has currently become an indispensable part of computer-aided engineering (CAE) and is utilized extensively in the analysis and design of many complex real-life systems. In other words, the finite element method (FEM), sometimes referred to as finite element analysis (FEA), is a computational technique employed in order to obtain approximate solutions to boundary value problems in engineering. In simple terms, a boundary value problem is a mathematical problem in which one or more dependent variables must meet a differential equation everywhere in the spectrum a known domain of independent variables and satisfy specific conditions on the boundary of the domain. Boundary value problems are occasionally symbolized as field problems. The field is the domain of interest and frequently represents a physical structure. The field variables are the dependent variables of interest governed by a differential equation. The boundary conditions are the specified values of the field variables (or related variables such as derivatives) at the boundaries of the field. On the basis of the type of physical problem being analyzed, the variable fields may include, for example, physical displacement, temperature, stress, heat flux, and fluid velocity. The finite element method is effective in solving both straightforward linear static issues and extremely intricate nonlinear transient dynamic problems. FEA is a mature field that currently rests on rigorous mathematical fundamentals. Many powerful commercial software packages are presently available that allow its wide utilization in several industries. The FEM can be viewed clearly as a method for finding approximate solutions to partial differential equations as well as a tool for transforming partial differential equations into algebraic equations that are then conveniently solved [24-26]. The basic principles of analysis using the finite element method are shown in Fig. 7.

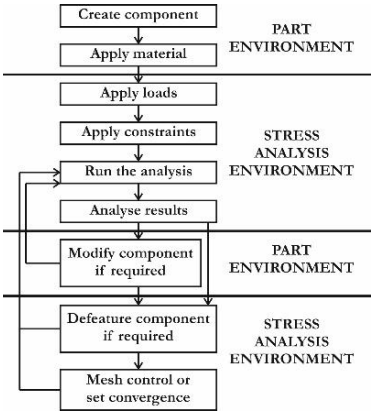


Fig. 7 *Finite element method analysis procedure* [27].

5.1 3D modeling of the end truck beam and determination of boundary conditions

The analysis of the end truck beam is performed in the working environment of the Ansys software. This software is employed to obtain the value of the maximum deflection of the end truck beam and to determine the value of the maximum bending stress. Catia V5 software from Dassault Systemes is utilized in order to create a 3D model of the end truck beam. In the working environment of this software, a spatial model of the end truck beam is designed (Fig. 8). The model model is created with regard to the dimensions (tab. 1) of the selected U40 end truck beam profile (Fig. 6). The length of designed beam is 510 mm.

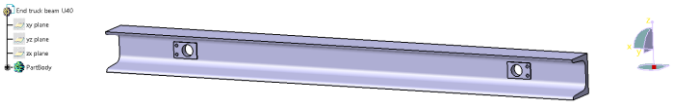


Fig. 8 *3D CAD model of the designed end truck beam U40.*

This created beam model is subsequently imported into the Ansys working environment. In addition, it is assigned the selected material S235, which has a yield strength of 235 MPa. The boundary conditions (Fig. 9) by means of the remote displacement function are further applied due to the analysis of the end truck beam model.

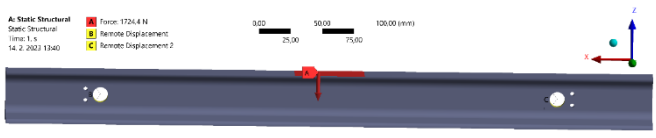


Fig. 9 *Boundary conditions applied to end truck beam model.*

The beam is supported on bearings of the pivots of two crane wheels. The beam is fixed on one pivot, and it can move in the x-axis direction on the other one. Moreover, there is an assumption of loosening in both bonds - rotation about the y-axis. An application surface is formed on the top flange of the beam, the dimensions of which are determined by the width of the main girder (the placement of the main girder on the end truck beam) and the width of the end truck beam for the reason that the end portion of the main beam is placed over the full width of the end truck beam. Figure 9 shows the created surface with its dimensions. The load F_Q of 1724.36 N value is applied to this surface. The acting load is determined based on formula (18):

$$F_Q = q_c \cdot b\,. \tag{18}$$

where F_Q – load acting on the end truck beam, q_c – distributed load calculated in (5), b – the width of the main girder of the bridge crane.

After substituting values into formula (16):

$$F_Q = 31.352 \cdot 55 = 1724.36\ \text{N}\,. \tag{18}$$

Subsequently, the end truck beam model is meshed (Fig. 10) using elements of the quadratic type. The size of the elements is 5 mm. The number of elements is 7841 and the number of nodes is 15791.

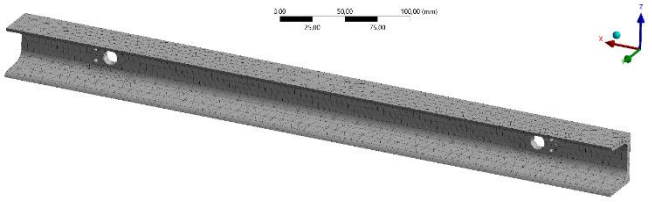


Fig. 10 *Meshed model of the end truck beam.*

5.2 Results of the FEM analysis of the designed end truck beam

In terms of FEM analysis results, the maximum bending stress and total deformation are crucial. For FEA, the value of Young's Modulus is $2.1 \cdot 10^5$ MPa and Poisson's ratio is 0.3.

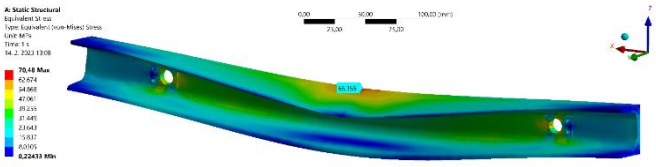


Fig. 11 *The resultant Von-Mises bending stresses arising on the end truck beam.*

Fig. 11 demonstrates that the maximum bending stress (Von Mises) is at the location of the main girder on the end truck beam, namely at the center of the end truck beam. The magnitude of obtained bending stress is 66.356 MPa. The value of computed maximum bending stress is marked and depicted in Fig. 11 in the blue box. Furthermore, Fig. 11 evidently demonstrates that the maximum stresses arise in the bonds.

The magnitude of the maximum deflection obtained by dint of the Ansys simulation program is 0.3823 mm. Fig. 12 shows the total deflection of the vehicle beam along with the value of the maximum deflection indicated by the red box. The maximum deflection is as expected at the placement of the main beam on the end truck beam.

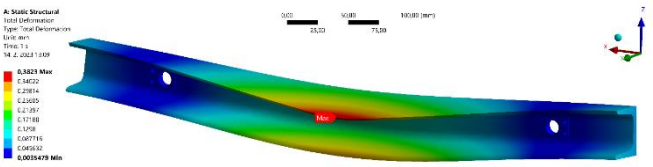


Fig. 12 *Total deformation of the end truck beam.*

Inasmuch as the value of the maximum bending stress is less than the value of the allowable stress, i.e., the condition given by formula (15) is met, it can be concluded that the proposed U40 S235JR end truck beam is suitable for the single girder bridge crane with a load capacity of 500 kg.

6. Conclusion

The main objectives of the addressed paper include an introduction to the issue of overhead cranes, especially their essential component, which is the end truck beam. The theoretical part of stated paper is focused on the introduction of one group of handling equipment, which are cranes, especially in terms of their division and use. Furthermore, this part deals with one of the most widely used groups of cranes, namely bridge cranes. On the one hand, it discusses bridge cranes in terms of their principle of operation, their operational specifications, their components, from the point of view of their design and utilization, on the other. The practical part of current paper concentrates on the end truck of bridge crane, especially the end truck beam. The predominant objectives are the design of the vehicle beam for the proposed single girder bridge crane with a load capacity of 500 kg and the strength check of the proposed end truck beam. On the basis of the input load data of the end truck beam and the dimensions of the main girder bearing area on the end truck beam, the minimum section modulus in bending was determined through the Allowable Stress Method as a critical parameter for the selection of the end truck beam. According to the calculated value of the minimum section modulus in bending, which was 1416.78 mm3, the U40 beam made of S235JR material was selected. The parameters of the section of chosen beam are given in Table 1. In addition, this beam was subsequently subjected to FEM analysis using Ansys software, where two parameters, namely maximum deflection and maximum bending stress, were examined. The value of the maximum deflection was 0.3823 mm, and this deflection occurred at the expected location, i.e., at the center of the beam of the end truck. The value of the maximum bending stress was 66.356 MPa. The values of the maximum bending stress and deflection are less than the permissible values. Thus, based on the numerical simulation results, it can be concluded that the proposed U40 vehicle beam is satisfactory in terms of strength and stiffness. Ultimately, the above calculations and results create a prerequisite for the possible production of the proposed end truck beam, which is a crucial component of the single girder bridge crane with a load capacity of 500 kg.

7. References

1. A. Bhatia, *Overview of Electric Overhead Traveling (EOT) Cranes: e-Book* (Scotts Valley, California, CreateSpace, 2014).
2. Kuľka J., M. Mantič, M. Pušk̈ár, *Bridge cranes* (In Slovak) (Košice, Technical university of Košice, 2018).
3. Patel, V., Types of Electric Overhead Travel Cranes (EOT Cranes), *Krishna Crane Engineers*, 2019.
4. Hrabovský, L., P. Vraník, *Transport and Handling systems, 2nd ed.* (In Czech) (Ostrava, VSB Technical university of Ostrava, 2017).
5. J. Pavliska, *Transport and Handling Equipment, 4th ed.* (in Czech) (Ostrava, VSB Technical university of Ostrava, 2004).
6. Hafid, A., D. Salimi, Ewitha, S. H. Nur, Analysis and Design of Crane Beam of Experimental Power Plant Turbine Building, *Jour. of Physics Conf. Ser.*, **1198**, 8 (2019).

7. Todorović, S., M. Rogić, Automation and Optimization of Poject Operations in the Bridge Crane Design Process, in: Proceedings of 10 Anniversary International Conference on Accomplishments in Electrical and Mechanical Engineering and Information Technology, 26.-28. May, 2011, Banja Luka, 801-807.
8. Ling, Z., M. Wang, J. Xia, S. Wang, X. Guo, Stress Analysis for the Critical Metal Structure of Bridge Crane, *IOP Conf. Series: Earth and Environ. Science*, **108**, 1-5 (2018).
9. Javeed Basha, G. MD., S.K. Rao, A crane hook's design and stress values calculation, *Europ. Jour. of Molec. and Clin. Medic.*, **4**, 1 (2017).
10. Brázda, R., J. Vyletělek, K. Skácel, P. Gűnther, J. Grabec, J. Žalčík, *Transport and Handling Machines* (In Czech) (Ostrava, VSB Technocal university of Ostrava, 2013).
11. A. Bhatia, *Electric Overhead Traveling (EOT) Cranes and Hoists* (PDH Online. 2020).
12. Molnár, D., M. Blatnický, J. Dižo, Design of a suitable cross-section of the main girder for a single girder bridge crane with a 500 kg load capacity, *Technolog*, **13**, 3 (2021).
13. Kulka, J., M. Mantic, G. Fedorko, V. Molnar, Failure analysis of increased rail wear of 200 tons foundry crane track, *Engine. Fail. Analysis*, **67**, 1-14 (2016).
14. Pavlović, G., M. Savković, N.B. Zdravković, G. Marković, Optimal Design of End Carriage Structures, *Mech. Transp. Commun.*, **19**, 3 (2021).
15. Pavlović, G., M. Savković, N. Zdravković, G. Marković, Optimization Design of End Carriage of the Single-Girder Bridge Crane Structure, *Mech. Transp. Commun.*, **18**, 3 (2020).
16. Li, H., H. Wu, Study on bridge structure of bridge crane, in: Proceedings of the 5th International Conference on Civil Engineering and Transportation, November, 2015, Guanzhou, China, 1776-1779.
17. TSOVERHEADCRANE, Double girder bridge crane, https://www.tsoverheadcrane.com/overhead-bridge-cranes, last accessed 2023/04/02.
18. DEMAG, End trucks, https://www.demag.sk/demag-pojazdy-dfw-l/, last accessed 2023/04/07.
19. Molnár, D., M. Blatnický, J. Dižo, Comparison of analytical and numerical approach in bridge crane solution, *Manuf. Techn.*, **22**, 2 (2022).
20. Molnár, D., M. Blatnický, J. Dižo, Design and strength analysis of a crane hook with a 500 kg lifting capacity, *Pern. Cont.*, **16**, 2 (2021).
21. Blatnický, M., D. Molnár, J. Dižo, Design of a suitable steel wire rope and rope drum for a single girder bridge crane with a load capacity of 500 kg, *Technolog*, **13**, 3 (2021).
22. STN 27 0103: Design of steel crane structures. Slovak Office of Standards, Metrology and Testing, Bratislava (1989).
23. FERONA, Catalog of steel profiles, https://online.ferona.cz/detail/28008/profil-u-valcovany-za-tepla-en-10365-u-40, last accessed 2023/04/13.
24. David V. Hutton, *Fundamentals of Finite Element Analysis*, (New York, McGraw-Hill, 2004).
25. Madenci, E., I. Guven, *The Finite Element Method and Applications in Engineering Using Ansys* (Berlin, Springer Verlag, 2015).
26. P. Seshu, *Textbook of Finite Element Analysis* (New Delhi, PHI Learning, 2012).
27. Suratkar, A., V. Shukla, 3D-modelling and finite element analysis of EOT crane, *IJERT*, **1**, 2 (2013).

Implementation of digital penetrometer S600 skokagro in the technology of precision and digital agriculture

Anatolii Kobets, Oleksii Derkach, Viktor Aulin, Dmytro Makarenko, Oleh Serhiienko
Faculty of Engineering and Technology – Dnipro State Agrarian and Economic University, Ukraine
e-mail: addsau@gmail.com, fly-makd@yandex.ua

Abstract: *The paper presents the method of combining the results of soil compaction, which were obtained by the penetrometer of Ukrainian production S 600, into the software of digital agriculture. For example, it is shown how to enter the obtained soil compaction data into the AFS software.*
KEYWORDS*: DIGITAL PETETROMETR, SOIL COMPACTION, DIGITAL FARMING, SOFTWARE.*

1. Introduction

As you know, the introduction of modern technologies for growing agricultural crops involves the solution of many tasks: reducing the use of resources, shortening the terms of sowing, care, harvesting; increasing soil fertility. The quality of the grown crop must meet world standards. Today, farmers of Ukraine use, along with traditional farming technologies, such as No-Tillage, Drill-Tillage, Strip-Till, Controll-Traffic. There is also the use of a mix of technologies within one agricultural enterprise. These technologies are effectively adapted to the conditions of agriculture in Ukraine. The main risk of agriculture before the war with the russian federation was the risk of low rainfall. Today, new limiting factors have appeared in agricultural production: mining of fields; reduced number of equipment and people. In order to obtain high yields with moderate expenditure of funds and other resources (human, material and technical), it is necessary to carry out technological operations in the shortest possible (short) period to compensate for these factors, powerful and high-performance machinery is used tractors: John Deere 8335R, John Deere 8345RT, Case IH STX 535/600 and others; combine harvesters Case IH 9420, Lexion 770, John Deere 670i; agricultural machines Horsch Maestro 36.5, Turbosem II 19-60, Ecolo-Tiger-730 and many other various machines. The use of unmanned aerial vehicles to perform various tasks is increasing: surveying fields, determining field boundaries, researching the state of plant development, spraying crops with protective agents, etc.

However, the use of high-performance equipment has its drawbacks - it is a large mass of tractors, combines and agricultural equipment. There is a threat of yield reduction due to excessive soil compaction. For example, the depth of action of the compacting effect from the wheels of a grain harvester weighing 13 tons or more reaches a depth of 0.8 m [1]. In the case of using traditional agricultural technology - with intensive tillage - the latter is also constantly exposed to the negative impact of the mass of tractors. And the depth of cultivation, as a rule, does not exceed 30...32 cm. In addition, it is calculated that the length of the path (traces) traveled by a combine harvester equipped with a harvester with a width of 6 meters, which harvested a crop in a field with an area of 100 hectares, reaches 125 ... 166 km , depending on the method of movement on the field. This leads to the formation of the so-called "plow sole" - a very compacted layer of soil, which significantly slows down the penetration of moisture and air into the deeper layers of the soil, and vice versa.

High compaction of the soil, of course, will lead to a significant decrease in productivity and may even provoke the death of plants (Fig. 1).

Thus, modern agriculture, regardless of the technology of growing agricultural crops, is characterized by the use of high-performance equipment that has a lot of weight. Based on this, it is necessary to implement additional methods of soil compaction control.

1. Statement of the problem

In the conditions of the implementation of agricultural technologies, in which high-performance and heavy machinery units are used, it is necessary to use tools for quick control and analysis of soil density. The existing penetrometers of the mechanical type (Fig. 2) cannot satisfy the requirements of farmers, since with their help it is not possible to obtain complete, accurate and, most importantly, quick information about the state of the soil.



Fig. 1 *– Sunflower crops, which stopped developing due to over-compaction of the soil (proved by measurements).*



Fig. 2 *– Penetrometer of mechanical type. No GPS tethering.*

The advantages of such a penetrometer include low cost, compactness, and ease of use. Disadvantages include: lack of GPS connection, lack of GSM, impossibility of creating compaction maps. Such and similar devices today do not meet modern requirements and cannot be used in precision and digital farming systems.

Thus, the goal of the work is to integrate the software of digital tools for determining the amount of soil compaction into programs for conducting digital agriculture. To achieve the goal, it is necessary to solve the following tasks:

- to provide a scheme of implementation of the technology from the "point of measurement - to the application of the results in the technology of cultivation of rural areas". cultures";
- to develop a technology for fixing soil hardness measurement points;
- conduct experimental measurements.

2. Solving the task

To implement the first task, we developed a technological scheme for the interaction of the penetrometer with software for

precision and digital agriculture by recording and transmitting data using GPS and GSM communication. (Fig. 3).

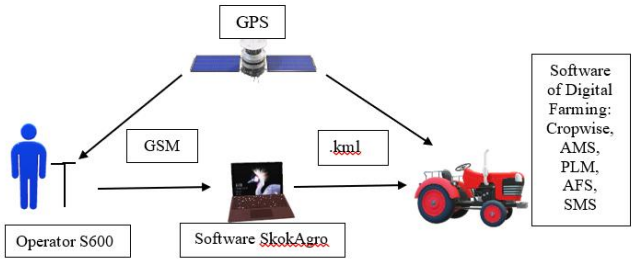


Fig. 3 – Scheme of data transfer of the amount of soil compaction from the moment of measurement to their entry into the task maps (prescriptions) in others software.

Such a technological scheme can be implemented using the digital penetrometer S600 of the Ukrainian manufacturer Skok Agro [2]. This penetrometer is equipped with a GPS receiver, GSM antenna and appropriate software for receiving, storing, analyzing and processing the received data (Fig. 4).

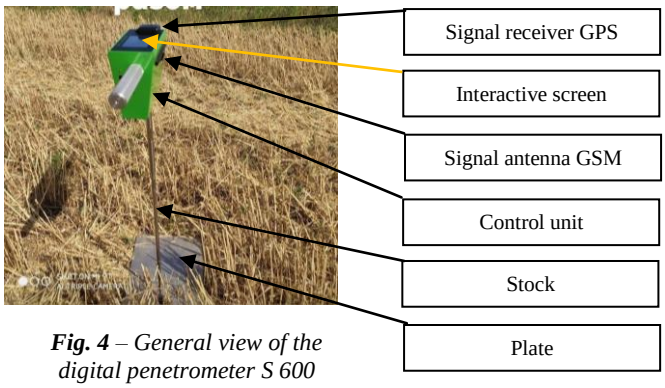


***Fig. 4** – General view of the digital penetrometer S 600*

A penetrometer measures soil hardness. This indicator is proportional to the compaction. The obtained hardness values are correlated with the amount of compaction. The received data of hardness (kPa) is transmitted to the server using GSM communication, from where they are read by the Skok Agro program, the interface of which is simple and convenient to use (Fig. 5). This software is connected to the Google Map service and has the following functions: "List of experiments" (measurements); "Reports on hardness" (completed works) and "Grid" [3]. Also, it is possible to limit the field on which hardness studies will be conducted with contours, which gives information about the area and configuration of the field. In the "Grid" mode, sampling points (points where soil hardness measurements will be taken) are automatically plotted on the map. Depending on the area of the field, you can choose the discreteness of measurements in the calculation: one measurement per 15 hectares; one measurement per 10 hectares, per 5 hectares or it is suggested to choose your own area smaller than 5 hectares (Fig. 6). The generated grid gives an understanding of where the operator needs to measure.



***Fig. 5** – General view of the Skok Agro interface.*

The operator who measures soil compaction must perform these measurements at the points determined by the Skok Agro software (Fig. 6).

In this case, the operator needed to find a measurement point on the field. Obviously, for this, it is necessary to match the coordinates of the points with another tracker, which must be installed on the operator's mobile device.

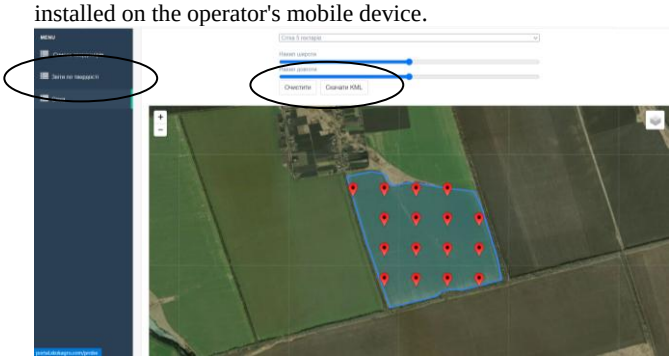


***Fig. 6** – Grid created automatically in Skok Agro software*

This task is implemented as follows. As can be seen from fig. 6, this information can be saved in a file with the extension ".kml". This file must be forwarded to the operator's e-mail box. The operator opens the received file in applications: GPX Viewer or Locus Map (Fig. 7 a, b), or any other application that accepts kml files. Thus, using this program and turning on the "Location" function on the smartphone, the operator moves along the field and combines the points of his location and the points on the field.



a) b)

***Fig. 7.** – Measurement points and operator movement tracker in applications: a - GPX Viewer; b - Locus Map*

After measuring the soil hardness at the specified points, the operator transmits the results to the server using GSM communication. These results are displayed in the Skok Agro software (Fig. 8). The hardness of the soil is determined at each given point to a depth of 60 cm with a resolution of 1 cm. Thus, we have a map of the soil hardness of the entire field to a depth of 60 cm.



***Fig. 8** – Soil hardness results of one of the agricultural enterprises on the border of Dnipropetrovska, Zaporizka and Donetska oblast (August 2021).*

Since the Skok Agro software has the ability to create files with the ".shape" extension, the results can be integrated into other precision and digital agriculture software.

3. Experimental part

14 measurements were made on the T18 experimental field of one of the agricultural enterprises. Crop cultivation technology - No Tillage since 2006. The obtained results were transferred to the Skok Agro portal. It was established that at a depth of up to 40 cm, the hardness of the soil is optimal and favorable for the development of the root system of plants (the effort of introducing the penetrometer pyramid into the soil was up to 3500 kPa). In fig. 9 shows the data of the soil hardness at a depth of 40 cm. In this case, such compaction is caused not by the action of the wheels of the machines, but by the soil's own weight. The received compaction data of the T18 field were transferred to AFS Software - and this was the beginning of the collection of information about the history of this field (Fig. 10).

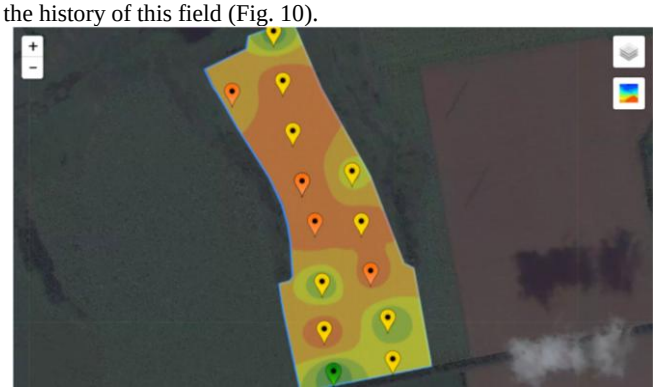


Fig. 9 – Results of soil hardness measurements of field T18.

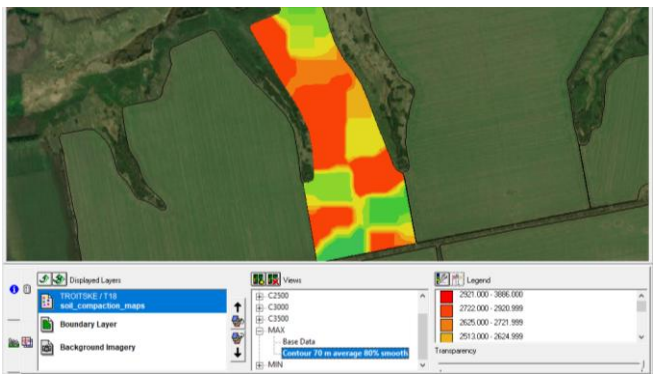


***Fig. 10** – T18 field compaction map after processing the results in AFS Software. Such maps can be built for different depths with a resolution of 5 cm.*

What gave us the definition of soil compaction? First, electronic maps of soil compaction help to adjust, for example, a deep loosener to the correct working depth. Each additional incorrectly identified centimeter of soil compaction, which is below the level of 20 cm, leads to an increase in fuel consumption by an average of 1 l/ha. But since the company where the research was conducted works on No-till technology, these soil compaction maps will go to the history of the field to further determine the zones of high, normal and low yield and their causes. In this case, we established that there is no excessive compaction of the soil in the root system development zone, and the effect of different soil density will not cause a significant negative effect on the crop. Therefore, for the agronomist there are other factors that will influence the formation of the crop: the availability of nutrients, soil moisture, etc. It is necessary to constantly monitor the NDVI index.

Note that in the process of implementing precision and digital farming technologies, at least three major factors play a significant role:

- amount of soil compaction;
- availability of soil moisture;
- availability of nutrients (organic and mineral).

The use of this penetrometer and software significantly accelerates the acquisition of data, their integration into other software [4] and ensures high accuracy of the obtained results.

* the authors express their gratitude to the owner of the production of S600 digital penetrometers and Skok Agro software - Serhiy Skok, who is currently defending the independence of Ukraine in the Armed Forces of Ukraine.

5. Literature

1. Pavliskii V.M., Nahirniy Yu.P., Melnyk I.I. Proektu-vannya tekhnolohichnykh system roslynnytstva. Ternopil: Zbruch, 2003. – 256 p.
2. Instruktsiia z expluatatsii tverdomira hruntu Skok Agro S 600. Versiia 1.3. 2019.
3. http://portal.skokagro.com/.
4. Технологія Topsoil-Mapper. [Електронний ресурс]. Режим доступу: https://www.topsoil-mapper.com/

Research and justification of automated monitoring of the microclimate of a farmer's greenhouse

Atihanov Aybek Kashkymbaevich[1], Bekaidarova Bakytkul Nurlybekovna[2]
Doctor of Technical Sciences, Professor, Kazakh National Agrarian Research University, Almaty, Republic of Kazakhstan[1]
Doctoral student of Kazakh National Agrarian Research University, Almaty, Republic of Kazakhstan[2]
E-mail: atihanov@mail.ru, baha@mail.ru

Abstract: *This article is a logical development of a previously implemented scientific project on the topic "Development of energy-saving technology for year-round production and processing of fruit and vegetable products based on multifunctional solar dryers-greenhouses" (State Registration No. 0111RK00488, inv. No. 0212RK01775, for 2012-2015, the amount of funding is 40 million tenge) under the budget program 055 "scientific and/or scientific and technical activities, subprogram 100 "Program-targeted financing, under the program "Targeted development of university science focused on innovative results".*

Goal. Substantiation and development of a system of automated remote monitoring of the microclimate (lighting) of a farmer's greenhouse, providing the most comfortable conditions for the growth and development of plants in the production of fruit and vegetable products using information technology to obtain a high yield of products at the lowest cost.

In winter, cultivated plants experience stress from a lack of natural light, which leads to a significant decrease in yield. In this regard, additional artificial lighting in the greenhouse allows the producer to extend the growing season and grow plants all year round or allows the producer to start sowing in early spring and continue the season until the first frost. Plants need about 10-12 hours of light to improve growth. When growing flowers or fruits, the additional need for light per day increases to 16 hours (5).

At the same time, the automation of this process will eliminate the concern that the lighting is in order and during its absence displays monitoring data on the display, or with the help of LEDs notifies about critical values of climatic parameters, or transmits data via the Internet to a tablet or phone for subsequent decision-making.

The article is aimed at meeting the demand of the population, farmers in the purchase of equipment adapted to local conditions, cheaper in cost and installation compared to analogues. The equipment attracts with its ease of manufacture and further operation.

Keywords: *AUTOMATED SYSTEMS, GREENHOUSE, MICROCLIMATE, MONITORING ALGORITHM, FARMING, MOBILE SMART APPLICATION, LIGHTING, PLATFORM*

1. Introduction

In greenhouses, the illumination to plants depends on the time of year and the state of the weather, in addition, the shadow side of the plants does not receive illumination compared to the side facing the light source. In accordance with this, a sufficient and necessary amount of light can be provided with even, comprehensive artificial lighting, depending on natural and weather conditions.

Recently, there has been a transition to more accurate and biologically based lighting standards for greenhouse plants. They isolate from the entire spectrum produced by the illumination lamp that part of the illumination spectrum that corresponds to the range of phytosynthetically active radiation (HEADLIGHTS).

In connection with the above, we consider it promising and expedient to develop a system of automated remote monitoring of the microclimate (lighting) of a farmer's greenhouse, providing the most comfortable conditions for the growth and development of plants in the production of fruit and vegetable products using information technology to obtain a high yield of products at the lowest cost.

Light is the main source of energy for photosynthesis. With an increase in the intensity of illumination, the quality of products improves, the content of vitamins in it increases, the amount of nitrates and nitrites harmful to the body decreases, the intensity of photosynthesis increases proportionally. For most plants, this pattern persists within the illumination intensity of 0.132 - 0.264 cal/sq. cm per minute (20 000 - 40 000 suite). With a further increase in the intensity of light, the intensity of photosynthesis begins to decrease, and then stops at a certain level.

Lighting in the greenhouse allows the manufacturer to extend the growing season. This allows you to grow plants all year round or allows the producer to start sowing in early spring and continue the season until the first frost. Plants need about 10-12 hours of light to improve growth. When growing flowers or fruits, the additional need for light per day increases to 16 hours.

In daylight, it would be rational to use devices capable of providing the greenhouse with the amount of light that the plant needs during the solstice. The density of the light energy supply should be from 400 to 1000 mmol per m2. In night lighting, photoperiodic lighting can be used. The energy supply density should be from 5 to 10 mmol per m2. It has a low spectrum of radius illumination (10).

The main idea is to create the necessary lighting for the growth and maintenance of cultivated plants in the greenhouse in order to obtain a high yield of fruit and vegetable products at the lowest labor costs, in particular, increasing the illumination of plants by 1%, increases the yield by 1%. In nature, this phenomenon is clearly observed on wild trees, which have the largest number of branches and leaves on the southern side of the trunk. Automation of the process will eliminate the concern that the lighting is in order and during its absence and displays monitoring data on the display, or using LEDs to notify about critical values of climatic parameters, or receive data via the Internet or on a tablet, phone for subsequent decision-making.

2. Materials and Methods

Greenhouses are designed to provide an optimal microclimate for the growth and development of plants. The greenhouse needs care: watering, maintaining the right temperature, light level.

It is necessary to realize the possibility of greenhouse management – to regulate the illumination of plants. You can control it using automation, or remotely (via the Internet or via a phone (tablet)).

In this project, we will create a smart-smart greenhouse that is able to control lighting, ventilation and automatic watering, has a real-time clock and GSM/GPRS Shield on board for remote control of the entire system, as well as for monitoring the current state.

The research will be based on generally accepted methods and a number of modified methods. The technology will also be tested on animated mockups with the inclusion of a system for monitoring humidity and ambient temperature "Sentinel-Control".

The information base of the project will consist of experimental and time-lapse observations of the technological process. Methods of applied systems theory, mathematical statistics, applied mechanics, computer programs MSExcel 2003, SPSS 16, Statistika 7, Autocad 2007, etc. will also be used.

This device will allow you to organize a fully automatic operation of your greenhouse or grow box (in case you grow vegetables / fruits at home in winter). The system allows you to control 3 important parameters at once: lighting, temperature, irrigation.

The main factors of plant growth and development: heat, light, air, water, nutrition. The sun is the main source of light for

plants. Only in the light do plants create complex organic compounds from water and carbon dioxide in the air. The duration of illumination greatly affects the growth and development of plants. The requirements for lighting conditions for plants are not the same. For southern plants, the length of daylight should be less than 12 hours (these are plants of a short day); for northern plants - more than 12 hours (these are plants of a long day). Artificially shortening or lengthening the daylight in the greenhouse, you can increase the yield and significantly improve its quality. The light acquires the greatest practical importance when growing seedlings and vegetables in greenhouses in winter. At this time, plants experience the greatest lack of light, since, firstly, it is the darkest time of the year and, secondly, a significant part of the light flux is absorbed passing through the glazed surface of the greenhouse and is shaded by grids.

If the greenhouse is located at 50 ° north latitude, then the duration of daylight in this region ranges from 8 hours in winter to about 16.4 hours in summer. For a 14-hour lighting mode in winter, it is necessary to illuminate up to 6 hours a day. With this mode, additional illumination is not necessary in summer.

In accordance with this, it follows that if you create the necessary conditions for the growth and maintenance of cultivated plants in a greenhouse (microclimate), then you can get a high yield of fruit and vegetable products with the least labor costs, in particular, increasing the illumination of plants by 1%, increases the yield by 1% .

One of the last facilities that was automated by SIN-Automatika is located in the Republic of Bashkortostan, near the city of Tuimazy. A greenhouse with a year-round growing cycle measuring 160 × 100 ×6.5 meters occupies 1.6 hectares. The greenhouse is equipped with 21 electric windows (70 m long). 36 fans are used for air recirculation.

44 groups of lamps are installed for additional lighting of plants, a total of 3,900 pieces with a power of 600 watts each.

Two panels with panel controllers ARIES SPK107 are equipped, mounted and put into operation to control engineering equipment. The controller maintains an archive that can be transferred to a USB flash drive for convenient data handling.

The greenhouse ACS can work both in manual and automatic mode. The system is connected to the OwenCloud service for remote parameter adjustments. The data is stored on the OwenCloud service for three months.

The XX IMEKO World Congress on Metrology for Green Growth on September 9, 14, 2012, in Bussan, Republic of Korea considered the topic "Greenhouses microclimate monitoring in real time based on a wireless sensor network and GIS".

In order to know and control the microclimate of the greenhouse, it is recommended to use intelligent sensor nodes with the possibility of wireless communication. ZigBee can be mentioned as one of the mandatory protocols associated with wireless sensor networks due to its low cost, low power consumption, extended range and architecture flexibility. Each sensor node is autonomous due to the use of energy from a solar cell through the battery charger circuit, taking into account also the power supply of the sensor and control node at night. Data from ZigBee network nodes are sent to an Ethernet wireless gateway connected to a computer running the LabVIEW application, which performs primary processing, and to a web-based geographic information system that provides information about the greenhouse microclimate.

China has created an application for smartphones that manages many processes (watering, fertilizing, temperature and humidity control) in a smart greenhouse. The area of the complex is 0.5 hectares.

The developers noted that the system delivers water and nutrients directly to the roots of plants. Every half hour, the system notifies about the microclimate in the greenhouse complex and identified pests of agricultural crops.

3. Results

At the latitude of the Almaty region, the average duration of daylight in the autumn and in these months is less than half of the average duration of May - June. In other words, in winter it is necessary to provide additional lighting for the plants cultivated in the greenhouse. And the time of winter illumination is comparable to the duration of a winter da

Figure 1 shows the dependence of the amount of solar radiation on the time of year in Almaty and Almaty region.

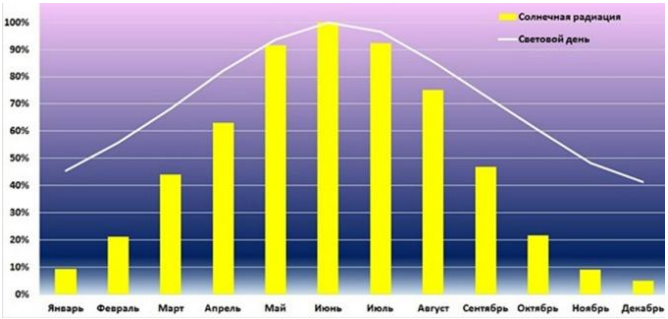


Fig.1 *The dependence of the magnitude of solar radiation on the time of year in Almaty and Almaty region.*

This means that in winter, plants in greenhouses will experience a significant shortage of natural light and, accordingly, this leads to a shortfall in the expected harvest.

The relative change in the activity of solar energy coming to Earth during the year differs significantly from the duration of daylight, although it has a similar character of seasonal change. The curve of relative dynamics of daylight duration at the latitude level of Almaty has the form of a more gentle dome compared to the dynamics of relative changes in solar radiation at the same latitude. Therefore, when the duration of daylight is halved in winter, the intensity of sunlight in winter is reduced by more than 10 times.

A significant disadvantage of most modern greenhouses is the inability to maintain optimal microclimate parameters by time of day. The issues of the level of solar intensity and the biological need for lighting during the cultivation of fruit and vegetable products and greenhouses in the Almaty region have not been sufficiently studied.

From the above it follows:

- A significant disadvantage of most modern greenhouses is the inability to maintain optimal microclimate parameters by time of day and for the entire vegetation period of plants.

- Insufficient consumption of sunlight can deprive a culture of normal development: a change in the shape and activity of growth; exclusion of fruiting (the plant simply will not bloom, and accordingly there will be no ovaries); unnatural elongation of cuttings and stems.

- Most of the energy comes from infrared radiation. It is advisable to place such a lamp away from plants, since there is a high probability of burns and overheating.

- Simply equipping a winter greenhouse with lighting is not enough. It is necessary to know the illumination standards in greenhouses, how much light per day is needed for a particular plant, as well as the possibility and territory that the structure can illuminate.

- In order for the lighting to be cost-effective, it is necessary to choose the right type of lamps. At the same time, energy costs depend on the geographical latitude in which the greenhouse is located, the time of year, the technology used for growing cucumbers and the degree of their precocity.

- It follows from the conducted studies that plants can have a short or long day of development and, accordingly, they require appropriate microclimate regimes and appropriate hardware equipment.

- The temperature of the indoor air in the greenhouse should vary depending on the crop turnover and the type of vegetables, and for the same vegetables – during growth and maturation, depending on the time of day.

- To create a Smart greenhouse, it is necessary to configure mobile or web applications according to the frequency of alerts about the operation of sensors in normal mode and emergency warnings about emergency situations.

- For each type of plant in the greenhouse, ultraviolet and infrared illumination of varying intensity is required, depending on the time of day and the growing season.

- The issues of using infrared radiation for heating greenhouses in winter have not been sufficiently studied.

- Modern farmers focus on the soil nutrition of plants, forgetting about its aerial nutrition, which can bring a larger harvest that gardeners could get if they carefully consider the process of photosynthesis in the greenhouse.

- The existing systems and equipment for creating a microclimate in protected ground are mainly focused on the production of crop production on an industrial scale, while they are not effective or adapted for small farm greenhouses with an area of up to 500 sq.m., while greenhouse management should not be complicated and distational.

Figure 2 shows the level of solar intensity during the growing of fruit and vegetable products of the greenhouse in the Almaty region. Through monitoring, the most comfortable conditions for the growth and development of plants in the production of fruit and vegetable products are provided. The monthly solar intensity and the biological need for lighting during the growing of tomatoes in greenhouses of the Almaty region are presented. It has been established that the intensity of sunlight in winter decreases by more than 10 times, therefore, additional illumination in the range ΔI and ΔII is necessary to enhance illumination (ΔI is a lack of illumination in autumn and winter, ΔII is a lack of illumination in winter and spring).



Fig.2 *Diagram of intensity and biological lighting needs during the period of growing tomatoes of fruit and vegetable products of the greenhouse in the Almaty region*

In our opinion, the regularities of this diagram can serve as a basis for the development of an appropriate automated program for monitoring the parameters of the greenhouse microclimate by the hour of the day and for the entire growing season of plants.

Fig.3 shows the proposed scheme of automation of the microclimate of a farm greenhouse

Automation of the microclimate of a farmer's greenhouse is proposed to be implemented through the Arduino platform - hardware and software with a pre-stitched loader in it, which allows you to load your program into a microcontroller without using separate hardware programmers. The microcontroller on the board is programmed using the Arduino language, based on the Wiring language (C like).

Arduino is a small board with its own processor and memory. The board also has a couple dozen contacts to which you can connect all possible components: light bulbs, sensors, motors, kettles, routers, magnetic door locks and in general everything that runs on electricity.

A program can be loaded into the Arduino processor that will control all these devices according to a given algorithm. Thus, you can create an infinite number of unique cool gadgets made with your own hands and according to your own idea.

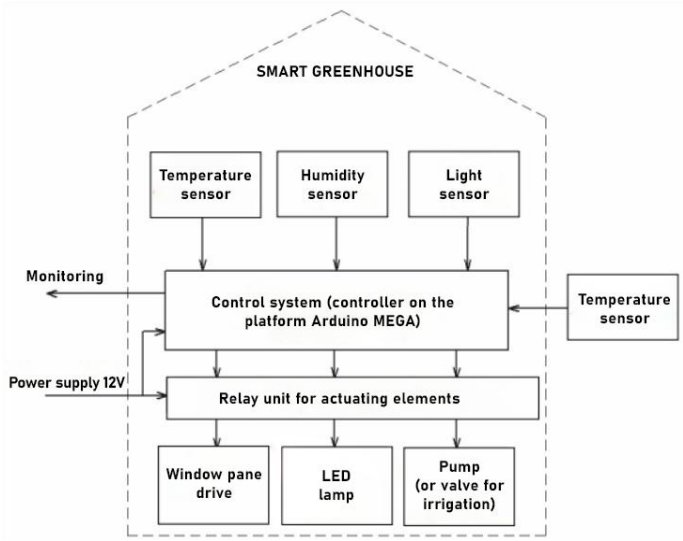


Fig.3 *Proposed. scheme of automation of the microclimate of a farm greenhouse*

The greenhouse control system is controlled by the Arduino central board, and works as follows: the received environmental data, temperature, air, humidity or lighting sensor is transmitted to the central controller (Arduino), which compares the current values with the set values. If any of the values does not match, then the actuator is activated to restore the optimal state. Next, Arduino sends data to a remote server for monitoring via the Internet.

If necessary, all the results of the equipment operation in an automated greenhouse can be visually tracked on a computer. The web interface can make it possible not only to monitor the readings of temperature, humidity and lighting sensors, but also to manage these very readings. It may also be possible to monitor the greenhouse via a webcam. The proposed program is easy to learn, and contains many sensors in its library. Before starting programming, it is necessary to draw a flowchart of the program. To do this, the free program DiagramDesigner 1.28 is used. The program code is written in the official development environment of ArduinoIDE 1.6.9.

The Arduino development environment consists of a built-in text editor of the program code, a message area, a text output window (console), a toolbar with buttons for frequently used commands and several menus. To download programs and communicate, the development environment is connected to the Arduino hardware.

A program written in the Arduino environment is designated as a sketch. The sketch is written in a text editor that has tools for cutting / pasting, searching / replacing text. While saving and exporting the project, explanations appear in the message area, and errors that have occurred may also be displayed. The text output window (console) shows Arduino messages including full error reports and other information. The toolbar buttons allow you to check and record the program, create, open and save a sketch.

The Arduino device programming language is based on C/C++. It is easy to learn, and at the moment Arduino is probably the most convenient way to program devices on microcontrollers.

The Arduino program consists of two functions:

setup(): the function is called once when the microcontroller starts.

loop(): the function is called after setup () in an infinite loop all the time the microcontroller is running.

CONCLUSION

The conducted review of studies on the creation of a microclimate in greenhouses allowed us to identify the main factors affecting the comfortable life of plants: temperature, illumination. The daily schedule is proposed according to the need, as well as for the

entire growing season. An automated platform has been selected that provides an optimal microclimate of a farmer's greenhouse. An algorithm for monitoring the parameters of the greenhouse microclimate has been developed. The technical components for the project implementation have been selected. A program for automating processes using a mobile application is proposed. A mobile application for monitoring the illumination of a farmer's greenhouse has been developed and its operation has been tested.

ACKNOWLEDGEMENT

We express gratitude to the Kazakh National Agrarian Research University for the contribution to the organization of laboratory laboratories for conducting practical experiments.

We express our sincere gratitude to Professor Plamen Ivanov Daskalov, PhD for your personal contribution to the project "Research and justification of automated monitoring of the microclimate of a farmer's greenhouse"

Sincerely, Atihanov Aibek Kashkymbaevich, Bekaidarova Bакytkγl Nurlybekkyzy

REFERENCES

ATIHANOV. A, K., DUISENOVASH.T., KARAIVANOVD.P.2018 Development to fequipmentforthestorage of soybeans with active ventilation.vi international scientific congress agricultural machinery. p.43-46 25– 28 June, Bulgaria. 2018.

ATIHANOV A.K. 2015 Solar dryer-greenhouse. RK Patent No.1318 for utility model, Ministry of Justice of the RK, 16.07.2015.

ARIELLE J. JOHNSON, ELLIOT MEYERSON, JOHN DE LA PARRA, TIMOTHY L. SAVAS, RISTOMIIKKULAINEN, CALEB B. HARPER. 2019 Flavor-cyber-agriculture: Optimization of plant metabolites in an open-source control environment through surrogate modeling // PLOS ONE. April. 2019.

B. Kassymbayev, A.Atihanov, D. Karaivanov, B.D. Kolev. 2014, 2015 A fruit drying mathematical model. International Journal of Pure and Applied MathematicsVolume101 No. 2 2015, 281-288. ISSN: 1311-8080 (printed version); ISSN: 1314-3395 (on-line version) (SCOPUS SJR 2014: 0,322) 2015, 2015.

BOOS G.V., PRIKUPETS L.B., ROZOVSKY E.I., STOLYAREVSKAYA R.I. 2017 Standardization of lighting equipment and installations for greenhouses. –No. 6 – pp. 69-74. 2017.

H.M. WOLLAEGER, E.S. RUNKLE. 2014 “Green light: Is it important for plant growth?”, Michigan State University Extension..[Online]. Available: http://msue.anr.msu.edu/news/green_light_is_it_important_for_plant_gr owth (5-25-2016).

KLEIMENOV M. 2019 Samsung developments for plant lighting // Semiconductor lighting engineering. – No. 2 – pp. 38-41. 2019.

KEMPKES F.L.K., HEMMING S., EDITED, CASTILLA N., VANKOOTEN O., SASE S., MENESES J.F, SCHNITZLER W.H., VANOS E. 2012 Calculation of NIR Effect on Greenhouse 130 Climate in Various Conditions // International Symposium on Greenhouse and Soilless Cultivation. – Lisbon; Portugal:ActaHorticulturae, - 2012. - P. 543-550 //http:www. webofknowledge.com.

LAMNATOU C, CHEMISANA D. 2013 Solar radiation manipulations and their role in greenhouse claddings: Fluorescent solarconcentrators, photoselective and other materials //Journal Citation Reports®. -2013. –P.175-190. DOI:10.1016/j.rser.2013.06.052.NOV 2013.ISSN:1364-0321. webofknowledge.com

NESIOLOVSKY O. G., ADAKIN R. D., SOTSKAYA I. M. 2021 Development of algorithms for energy-saving microclimate control (irrigation, lighting, heating, ventilation) in industrial greenhouses //improvement of electrical installations and power supply systems in agriculture.– pp. 26-32. 2021.

OVCHINNIKOV, I. K., AND R. P. PAVLIKOV. 2021 "Development of a model of a "smart" greenhouse with the possibility of remote control." 43-44. 2021.

PRIKUPETS L.B., BOOS G.V., TEREKHOV V.G., TARAKANOV I.G. 2018 Investigation of the effect of radiation in various ranges of the headlight area on the productivity and biochemical composition of biomass of salad-green crops // Svetotekhnika.–No. 5 – pp. 6-12. - 2018.

PETIN V.A. 2014 Projects using the Arduino controller / V.A. Petin - St. Petersburg: BHV-Petersburg.- 400c, 2014.

R. PARADISO, E. MEINEN, J. F.H. SNEL, P. DE VISSER, W. V. IEPEREN, S. W. HOGEWONING, L. F.M. 2011 Marcelis, Spectral dependence of photosynthesis and light absorptance in single leaves and canopy in rose, ScientiaHorticulturae 127,pp. 548–554, 2011.

SASHINA A., MAIDANOV N., BEREZINA A. 2022 Smart greenhouse "SmartGreenhouse" //From the green campus to the green city. – pp. 46-63, 2022.

SULEYMANOV V.O., MEZENTSEV E.E.,KOZLOV A.V. 2021 Naming of LED lamps for greenhouse lighting. Topical issues of science and economy: New challenges and solutions Collection of Materials LV Student Scientific and Practical Conference. Volume Part 2, Pages: 710-713, 2021.

STOLYAREVSKAYA R.I., ROZOVSKY E.I. 2017 The current state and development of photometry of lighting devices // Lighting engineering. – No. 4. – p. 4-13, 2017.

SACILIK K., KESKIN R., ELICIN A. 2006 Mathematical modelling of solar tunnel drying of thin layer organic tomato // Journal of Food Engineering. - Vol. 73, №3. - P. 231-238, 2006.

SETHI V.P., SUMATHY K., LEE C., PAL D.S. 2013 Thermal modeling aspects of solar greenhouse microclimate control: A review on heating technologies // Journal Citation Reports®. – 2013, October. – P. 56-82 // http:www.webofknowledge.com. 10.1016/j.solener..06.034.

TEREKHOV V. G. Method of experimental determination of optimal parameters of technological lighting in conditions of light culture of green plants. Abstract, Moscow, pp. 15-18, 2020.

THIEBLEMONT H., HAGHIGHAT F. 2016 Thermal Energy Storage for Building Load Management: Application to Electrically Heated Floor. // Applied Sciences, 2016.

GREENHOUSE PRACTICE: "TOMATOES: TECHNOLOGY" (DIGEST OF THE JOURNAL "MIRTEPLITS"). MOSCOW: NAUKA, — 290 P. 2018.

Comparison of tillage technologies in relation to changes in soil properties using soil biostimulation

Pavol Findura[1], Miroslav Prístavka[1*], Hristo Beloev[2], Plamen Kangalov[2], Mitko Nikolov[2],
Maciej Kubon[3], Urszula Malaga-Tobola[3], Erik Lavrík[1], Maksym Stankevych[1]
Slovak University of Agriculture in Nitra, Slovakia[1]
Angel Kanchev University of Ruse, Ruse, Bulgaria[2]
University of Agriculture in Krakow, Poland[3]
miroslav.pristavka@uniag.sk

Abstract: Climate change is causing problems for farmers almost throughout Europe, particularly in the area of soil drought. The current soil situation in Slovakia and Europe is not favourable. Declining cattle numbers are causing a shortage of organic fertiliser, soil degradation is occurring, as is soil compaction with high weight agricultural machinery causing changes in the bulk density of the soil and its penetrometric resistance. The aim of this paper is to point out the possibilities of prevention against soil degradation. In this paper we compare the effect of conventional technology and soil conservation technology in combination with soil biostimulation on the change of soil condition.
Keywords*:* SOIL, BIOSTIMULATION, PENETROMETRIC RESISTANCE

1. Introduction

The choice of tillage technology is related to the water in the soil, which also influences the formation of future crops. Soil compaction, erosion and slump formation are the factors that contribute most to and lead to soil degradation, with a significant impact on soil properties. There is a need for a complete rethink on this issue, which has become more and more topical over time and has perhaps never been more topical than it is today, when the main objective is gradually becoming to increase fertility, in line with the choice of soil minimisation technologies that take account of the soil conditions. Depending on the agricultural machinery used, the soil structure and the size of soil aggregates change. Deep loosening improves the condition of compacted layers and organic fertilization increases aggregate stability and soil bearing capacity (Estler et al., 1996, Nadykto et al., 2022).

Tillage practices vary according to the type and condition of the soil after the previous crop, as well as local conditions. We have problems with heavy soils that can only be worked well within the moisture range, while light soils can be worked at higher moisture levels without risk of damaging the soil structure. The choice of the appropriate tillage technology is also influenced by climatic conditions (Páltik et al., 2005, Bulgakov et al., 2022).

We place opposite requirements on the soil as a driving track than on the soil that is to be used for germination and development of cultivated plants. We require that the rolling resistance of the wheels is minimal, which can be achieved by digging them into the soil as little as possible, i.e. the soil must have a high load-bearing capacity. Since the transfer of power from the energy means to the agricultural machine is mostly through the transfer of tensile force, the wheels exert both normal and tangential forces on the soil (Mishta et al., 1993, Findura et al., 2022). The normal forces cause compressive loading of the soil within the contact area of the wheels with the soil, which reduces the porosity and increases the bulk density of the soil. As the engine power of the power vehicle increases, the more normal force is needed to generate the required tractor pulling force. The tangential forces generated, due to friction between the wheel and the soil as well as due to the shaped tyre profiles, cause pressure and shear loads that induce horizontal displacements in the soil and loss of energy, mainly due to the slipping of the driving wheels and the consequent devastation of the soil structure (Findura., 2020).

2. Materials and Methods

Measurements for the dissertation were carried out in the company AGROTECHNA s.r.o. Michalovce. The enterprise is located in the Košice region in the district of Michalovce in the cadastre of the village Stretavka. It is an enterprise focused on crop production. The enterprise farms in four cadastral territories. The specific location of the enterprise is that it is situated between the confluences of three rivers Uh, Laborec, Čierna Voda. The altitude of the farm Stretavka is 102 m above sea level. The farm itself is also affected by groundwater which causes high groundwater table on some plots. Under the given conditions, years with lower rainfall are more favourable for crop production. Soil heterogeneity map of soil block - Stretavka (BPEJ 0311002, H/HP or PH/PH, medium soil) 3 variants:

1 - Soil protection technology with deep loosening + auxiliary soil preparation NEOSOL

2 - Conventional technology (ploughing) + NEOSOL soil conditioner

3 - conventional technology (ploughing).



Fig.1 Satellite photo of the investigated experimental plots

The experimental part of the thesis further includes:

- Measurement of fuel consumption in cultivation without and with the use of conditioning agents

- soil structure.

- Measurement of soil penetrometric resistance,

- Measurement of soil infiltration,

- Measurement of soil moisture,

- Measurement of pulling power in relation to fuel consumption,

- Determination of surface coverage by plant residues,

- Determination of yield of selected crops.

The measurements of the tensile resistance were carried out during the ploughing operation with a 5 radial plough to a depth of 30 cm by a strain gauge device in both parts of the plot, namely the treated preparation and the control part. The tensile resistance measurement kit included measuring instruments and equipment (Zetor 162 45 tractor, 5PHX 35 semi-trailer plough and Hottinger Baldwin Messtechnik Spider-8 measuring system. The measurements were carried out on the plot and with the treated preparation and on the control section. The equipment recorded the tensile resistance value in kN at 0.2 s intervals.



Fig.2 HBM Spider 8 with computer for transmission of recorded data, mechanical part of the tensile resistance measuring device

Fuel consumption was measured in two ways. The first way was by using the EDMeco measuring device which automatically wrote the consumption data to a USB memory transfer medium. The second way of measuring fuel consumption consisted in filling the fuel to the edge of the measuring cylinder, after which the given working operation was performed on the measuring set. After the operation was completed, the measuring cylinder was again filled to the brim and the difference between the fuel consumed and the fuel topped up was the consumption which was entered into the tables.

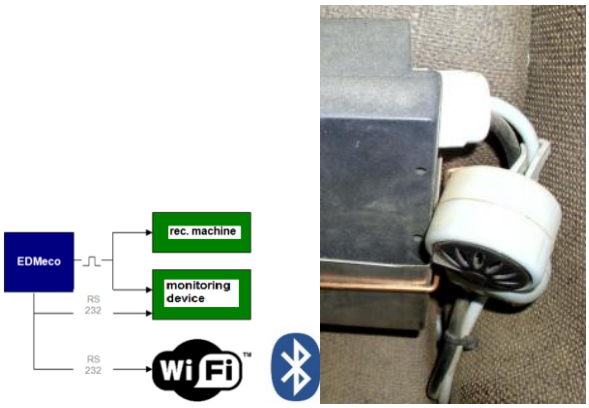


Fig.3 Schematic of EDMeco system communication with recorder, monitoring device and remote access

We also monitored yields from individual plots at harvest to compare the different options.

3. Results

We monitored the individual variants over four years. In the spring of 2022, moisture content ranged from 20.8% to 22.7% when sampling the 25 cm depth variant. Compared to spring 2020, moisture conditions are more favorable. Based on the measurements, we can conclude that the difference in moisture content between the variants was negligible for the control and reached an average value of 21.2%, for the plough variant with biostimulant it reached an average value of 22.3%, for the soil conservation technology with biostimulant it reached an average value of 21.6%. However, when evaluating the bulk density, I can state that in spring 2018 there was a trend of its decrease for all variants. Comparing the conventional technology and the soil conservation technology with soil stimulation applied in spring 2018, we can state that for the conventional technology a positive change in the decrease in bulk density to 1.38 $t.m^{-3}$ was recorded, for the soil conservation technology with biostimulant we achieved an average value of 1.40 $t.m^{-3}$.

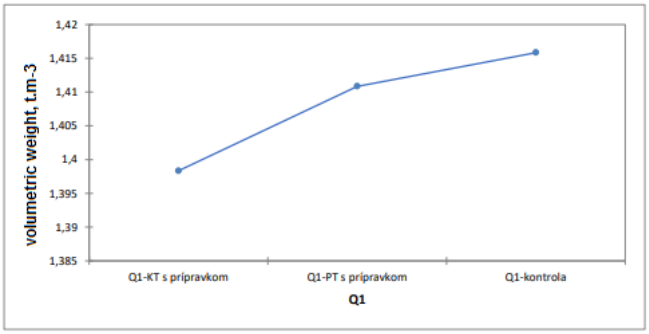


Fig.4 Comparison of the averages of the volumetric masses of the different variants as a function of time

On the basis of this test, which compares the different variants with each other, we can conclude that when comparing the bulk density of the conventional technology and the control, the p-value is less than 0.05, which demonstrates the demonstrability of the effect of the biostimulant on the change in bulk density. When comparing the soil conservation technology with the biostimulant and the control, we came up with a value of 0.0496 which is also a demonstrable difference.

Tab.1 Results of Fisher's LSD test for soil bulk density

	Difference	Standard deviation	Critical value	P > Diffe.	Signal difference
Check vs KT	0.0175	2.0556	2.0345	0.0478	**Yes**
Check vs PT	0.0050	0.5873	2.0345	0.0496	**Yes**
PT vs KT	0.0125	1.83	2.0345	0.1515	No

Control measurements, confirm the results of our measurements. In the soil treatment area, the penetrometric resistance is lower and from 210 mm onwards for all three variants the penetrometric resistance increases. For the control, the progression is the same only with higher values. This fact confirms the positive effect of the biostimulant on the soil aggregates. A comparison of the same tillage treatment between the control and the application of the biostimulant showed a difference of 1.55 MPa. On the basis of the measured data, we can conclude that the largest difference was observed between the control and the use of soil conservation technology with biostimulant, namely 2.05 MPa.

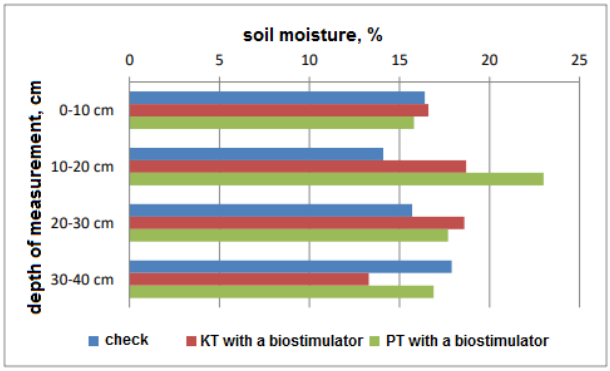


Fig.5 Measurement of soil moisture in individual depth variations

Based on our measurements and processing of the results, we can say with certainty that we can talk about a reduction in fuel consumption per hectare. Strain gauge force sensors which recorded the amount of tensile resistance and the Hottinger Baldwin Messtechnik Spider-8 measuring unit. We measured lower values in the plot where the product was applied. During the Neosol pass we recorded a total calculated maximum tensile resistance of 40 057 kN. The average value of the recalculated maximum tensile strength on the control section is 58 371 kN, which was a difference of 18 314 kN compared to the preparation. Comparison of the measured and recalculated values of the tensile resistance of the implement in the soil and the total labour requirement showed that the workability of the soil was significantly better in the preparation treated part of the plot compared to the control part of the plot. A simple analysis of these results confirms the fact that the improved biological activity function and consequently soil structure resulted in a 26.76% reduction in tensile resistance compared to the plot where the product was not applied, a reduction in total labour requirement of approximately 11.5% and a reduction in diesel consumption per hectare of approximately 35% in the year of measurement.

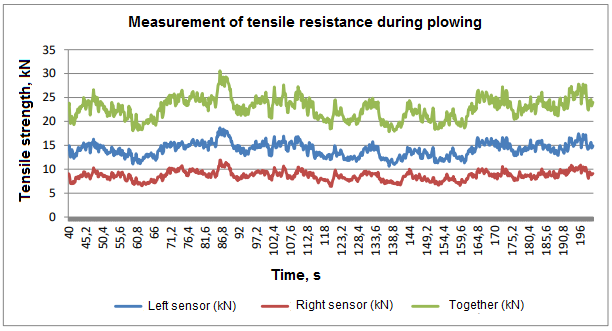


Fig.6 Excerpt from tensile force measurement record

Based on the results obtained for the soil treatment, we can conclude that in 2020, the conventional technology with biostimulation had a 10.1% lower fuel consumption compared to the control. For the soil conservation technology with biostimulation in 2016, the difference compared to the control was only 0.2%. In 2021, between conventional technology with biostimulation and control (KT), the difference in favour of Neosol was only 7% and between control and soil conservation technology with biostimulation the difference was up to 40.6%.

CONCLUSION

The main objective of the scientific article is to evaluate the results of research on the impact of biostimulation in conventional and conservation tillage on the change of soil condition, i.e. the change of physical-mechanical properties of the soil, soil resistivity, energy and fuel consumption and fertility elements. The modified cropping system consisted mainly of the application of a biostimulant at a fixed rate for several years in succession. On the basis of the results obtained, we can conclude that the use of soil conservation technology in combination with soil biostimulation has a positive effect on the change in soil condition and on soil water conservation.

ACKNOWLEDGEMENT

This paper was created with financial support of the grant project Vega no. 1/0102/21" Reducing chemical loads and degradation of agricultural and forestry soils by selecting appropriate agri-technology with regard to climate change".

This paper was created with financial support of the grant project Kega no. 016SPU-4/2021" Implementation of modern educational approaches and tools to enhance creativity and practical skills of graduates with special focus on agricultural and forestry science using"

This paper was created with financial support of the grant project Sustainable smart farming systems taking into account the future challenges of 313011W112, co-financed by the European Regional Development Fund.

This publication is the result of the project implementation: „Scientific support of climate change adaptation in agriculture and mitigation of soil degradation" (ITMS2014+ 313011W580) supported by the Integrated Infrastructure Operational Programme funded by the ERDF.

REFERENCES

ESTLER, M. – KNITTEL, H. – ZELTER, E. 1996 Praktische Bodenarbeitung. 2. vyd. Frankfurt am Main: DLG Verlags-GmbH, 253 s. ISBN 3-7690-0529-5

FINDURA, P. - ŠINDELKOVÁ, I. - RUSINEK, R. - KARAMI, H. - GANCARZ, M., 2022. Determination of the influence of biostimulants on soil properties and field crop yields. In International agrophysics. 36, 1 (2022), s. 83--91. ISSN 0236-8722.

BULGAKOV, V., M.- FINDURA, P.- NADYKTO, V.- KYURCHEV, V. - TIKHOVOD, M., 2022. Experimental study of two fallow field treatment influence methods on soil moisture dynamics. In Acta technologica agriculturae. 25, 4 (2022), s. 176-182. ISSN 1335-2555.

NADYKTO, V.- FINDURA, P.- KYURCHEV, V.- OREL, O., 2022. Influence of biodiesel on performance of machine-tractor units. In Acta technologica agriculturae. 25, 1 (2022), s. 7--12. ISSN 1335-2555.

PÁLTIK, J., FINDURA, P., POLC, M., 2005. Stroje pre rastlinnú xvýrobu. 1. vyd. Nitra: SPU, 2005. 241 s. ISBN 80-8069-200-9.

MALEŘ, J. 1996, Post-harvest treatment of grains. Vyd. 1. Prague: Institute of Education of the Ministry of Agriculture of the Czech Republic,1996a, 57 s. Mechanizace. ISBN 80-710-5112-8.

MALEŘ, J. 1996 Grain storage. 1st edition. Prague: Institute of Education Ministry of Agriculture of the Czech Republic,1996b, 58 s. Mechanizace. ISBN 80-710-5113-6

MAREČEK, J. 2009 Conditions for maintaining the quality of the grain at harvest. Available online: http://www.agroporadenstvo.sk

RIGO, I. 2016 Aspects of drying of selected agricultural crops. Diploma thesis, SUA in Nitra, 51 s.

Methodical approach to determine the gamma-percentage resource of aggregates and units of forklift trucks

Ivan Bitunski, Miho Mihov
Agricultural Academy, Sofia

Abstract: *Increasing the efficiency of machine usage for transport services in agricultural holdings can be achieved by creating stocks of aggregates and units in company warehouses based on a predetermined gamma-percentage of available resources.*
This study proposes a methodical approach to determine the 80% of gamma-percentage resource for forklift elements, considering both known and unknown distribution laws for their resources. It includes truncated and repeatedly truncated samples.
The results obtained from this study can be utilized for planning purposes and establishing stock levels to ensure the operational readiness of Bulgarian forklifts.
KEY WORDS: *RESOURCE, GAMMA-RESOURCE, SPARE PARTS, STOCKS, MACHINES, PRODUCTION, WORKING CONDITION, EXTRACT.*

It is well-established that the costs of maintaining a spare parts reserve for machines are significantly lower than the potential losses incurred from their unavailability. Consequently, a significant portion of the inventory is held not out of necessity, but as a precautionary measure. Spare parts warehouses often maintain excess stock due to concerns about shortages.

However, maintaining such reserves involves high costs and ties up working capital. The challenge lies in reducing inventory levels while ensuring high-demand fulfillment.

To address this challenge, it is crucial to know about the resource allocation of machine elements in use. By creating reserves based on a predetermined gamma-percentage resource of core components, efficiency in utilizing machines for transport services in agricultural bases can be improved.

The gamma-percentage resource represents the lower confidence limit of resource dispersion at a one-sided confidence boundary.

$$\beta_0 = \gamma \text{ , where } \gamma = \frac{\gamma\,\%}{100}.$$

When a theoretical distribution law of resource allocation for elements is known, the 80% gamma resource can be calculated using established dependencies,

- normal distribution law.

$$t_\gamma = \bar{t} - U_k(0{,}8).\sigma \quad ,$$

where $\bar{t}$ is the average resource of the element;

$U_k(0{,}8)$ - the quantile of the distribution law;

σ - the assessment of the standard deviation.

- For the Weibull distribution law

$$t_\gamma = U_k(1-0{,}8).a + c,$$

Where “a “ и “c” are parameters of the distribution law;

$U_k(1-0{,}8)$ - the quantile of the distribution law.

Than the 80% gamma-resource of the forklift engine is:

$$t_\gamma = U_k(1-0{,}8).a + c = 0{,}567.23229 + 0 = 13171$$

where a=23229 is parameter of the distribution law;

$U_k(1-0{,}8)$ =0,567 the quantile of the distribution law;

c =0 is parameter of the distribution law.

In this manner, the 80% gamma resource for all primary components of the forklifts is determined when the resource distribution law is known. The obtained results are presented in Table 5.

In cases where the resource distribution law is unknown and a truncated sample is used- if, at the end of the observation period, more than 20% of the objects from the initial sample have exhausted their resource, while the utilization of all remaining objects in working condition surpasses that of the objects reaching the limit state, these steps are followed to determine the 80% gamma resource is performed in two stages:

- The utilization of all tested objects is arranged in ascending order.
- The member of the variation sequence corresponding to the 80% gamma resource is determined using the provided formula.

$$N_{80\%} = \frac{N.80}{100} + 0{,}5 \quad ,$$

where $N_{80\%}$ is the number of the member in the variation sequence whose utilization corresponds to the 80% gamma resource;

N - the number of members in the variation sequence / the number of objects participating in the observation, no.

If a fractional number is obtained, an adjustment is made to the calculated result:

$$T_{80\%} = T_i - \left(T_i - T_{i+1}\right)\left(N_{80\%} - N_i\right) \quad ,$$

$$N_{i+1} = N_{80\%} = N_i$$

where N_{i+1} и N_i The respective nearest larger and smaller consecutive members of the variation sequence relative to the obtained number N=80%;

T_i - the resource of the object corresponding to the consecutive member in the variation sequence;

T_{i+1} - The resource of the object corresponding to the consecutive member in the variation sequence

Determining the 80% gamma resource of the forklift's hydraulic cylinder - in the case of a truncated sample

Initial information - hydraulic cylinder

Table 1

Failures, liters of primary fuel		Stopped during observation, liters of primary fuel	
1.	1 086	1.	24 282
2.	9 395	2.	27 942
3.	11 797	3.	29 409
4.	17 457	4.	30 120
5.	20 971	5.	31 170
6.	22 510	6.	35 156
7.	24 084	7.	37 090
8.		8.	41 010

- The utilization of the failed and stopped elements is organized in a descending order:

Table 2

Failures, liters of primary fuel		Stopped during observation, liters of primary fuel	
1.	1 086	8.	24 282
2.	9 395	9.	27 942
3.	11 797	10.	29 409
4.	17 457	11.	30 120
5.	20 971	12.	31 170
6.	22 510	13.	35 156
7.	24 084	14.	37 090
		15.	41 010

- the member of the variation sequence with the 80% gamma resource is determined,

$$N_{80\%} = \frac{15.80}{100} + 0{,}5 = 10{,}1$$

- determining of the 80% resource of the element,

$$T_{80\%} = 29409 - (29409 - 30120)(10{,}1 - 10) = 29480$$

liters fuel.

In the case of an unknown resource distribution law and multiple truncated samples - when the observations of N elements are terminated, some of them have exhausted their resource at utilization $t_1,\ t_2,\ \ldots\ t_n$. The other part remained elements in working condition with utilization $T_1,\ T_2,\ \ldots\ T_{N-n}$, where the utilizations of some elements that have not exhausted their resource can be greater than those of the elements that have exhausted their resource.

In this scenario, the determination of the 80% gamma resource is carried out in the following sequence:

- The utilization of the remaining elements in working condition is arranged in ascending order, $T_1 < T_2 < \ \ldots\ < T_k$;

- The intervals of utilization are numbered as follows: 1st interval - from 0 to T1; 2nd interval - from T1 to T2; up to the k-th interval - from Tk-1 to Tk;

- q_1- represents the number of elements for which the observation was terminated at utilization T_1; q_2- represents the number of elements for which the observation was terminated at utilization T_2; and $q_к$- represents the number of elements for which the observation was terminated at utilization $T_к$;

- n_1 represents the number of elements that have exhausted their resource in the first utilization interval (0 . . . T_1); n_2 epresents the number of elements that have exhausted their resource in the second utilization interval (T_1 . . . T_2); and $n_к$ epresents the number of elements that have exhausted their resource in the k-th utilization interval ($T_{к-1}$. . . $T_к$);

- N_1 represents the number of elements that continue operating after utilization T_1; N_2 represents the number of elements that continue operating after utilization T_2; and $N_к$ epresents the number of elements that continue operating after utilization $T_к$;

In accordance with the adopted notations, we determine the number of operational elements after each utilization interval:

$$N_1 = N - n_1 - q_1 \quad ;$$

$$N_2 = N_1 - n_2 - q_2 \quad ;$$

. . . . . .

$$N_k = N_{k-1} - n_k - q_k \quad ;$$

$$N_k = n_{k+1} \quad ;$$

$$n = n_1 + n_2 + \ \ldots\ + n_{k+1} \quad ;$$

- probabilities of failure-free operation $P(t_i)$ for the failed elements at utilizations: $t_1,\ t_2,\ \ldots\ t_n$ are determined using the following formulas:

$$P(t_1) = 1 - \delta_1 \quad ;$$

$$P(t_2) = P(t_1) - \delta_2 \quad ;$$

. . . . .

$$P(t_n) = P(t_{n-1}) - \delta_n \quad ;$$

The value of δ_1 in the previous formula with $t_1 < T_1$, is determined by,

$$\delta_1 = (N+1)^{-1} \quad .$$

If there are utilizations of non-failed elements $t_{i-1}\ \ and\ \ t_i$ (remaining in working condition) between the utilizations , and the maximum of those utilizations is denoted as Ti , then

$$\delta_1 = \frac{P(t_{i-1})}{N_i} \quad ,$$

where N_i e the number of elements remaining in working condition after the utilization T_i.

After calculating the values of δ_i for all utilizations t_i and T_i, including both failed and non-failed elements, we determine the failure probabilities $P(t_1)$ and $P(T_1)$. We find two adjacent utilizations (denoted as R_{i-1} and R_1) that satisfy the condition $P(R_{i-1}) > 0{,}8$ and $P(R_i) < 0{,}8$, and then we calculate the 80% gamma resource using the interpolation formula.

$$T_{80\%} = R_{i-1} + \left(R_i - R_{i-1}\right)\frac{P(R_{i-1} - 0{,}8)}{P(R_{i-1}) - P(R_i)} \quad .$$

To determine the 80% gamma resource of the engine cylinder head, considering multiple truncated samples

Initial information - engine cylinder head

Table 3

Failures, liters of primary fuel				Stopped during observation, liters of primary fuel					
1.	10 460	10.	24 670	1.	15 515	10.	22 850	19.	27 150
2.	11 153	11.	26 735	2.	15 571	11.	23 552	20.	27 303
3.	11 362	12.	34 330	3.	20 514	12.	23 915	21.	27 510
4.	12 016	13.	34 610	4.	21 023	13.	25 393	22.	29 291
5.	12 810			5.	21 481	14.	25 480	23.	30 005
6.	13 642			6.	21 841	15.	25 531	24.	30 669
7.	13850			7.	22 000	16.	25 624	25.	32 630
8.	14 119			8.	22 133	17.	25 724	26.	36 800
9.	23 606			9.	22 715	18.	26 909		

- determination of the number of elements in the individual intervals of the production:

Table 4

N_1=39 - 8 - 0 =31	N_{10}=23 - 0 - 1 =22	N_{19}=12 - 1 - 1 =10
N_2=31 - 0 - 1 =30	N_{11}=22- 0 - 1 =21	N_{20}=10 - 0 - 1 =9
N_3=30 - 0 - 1 =29	N_{12}=21 - 1 - 1 =19	N_{21}=9 - 0 - 1 = 8
N_4=29 - 0 - 1 =28	N_{13}=19 - 1 - 1 =17	N_{22}=8 - 0 - 1 = 7
N_5=28 - 0 - 1 =27	N_{14}=17 - 0 - 1 =16	N_{23}=7 - 0 - 1 = 6
N_6=27 - 0 - 1 =26	N_{15}=16 - 0 - 1 =15	N_{24}=6 - 0 - 1 = 5
N_7=26 - 0 - 1 =25	N_{16}=15 - 0 - 1 =14	N_{25}=5 - 0 - 1 = 4
N_8=25 - 0 - 1 =24	N_{17}=14 - 0 - 1 =13	N_{26}=4 - 2 - 1 = 1
N_9=24 - 0 - 1 =23	N_{18}=13 - 0 - 1 =12	

- determination the probability of trouble-free operation during production "T_1" of the elements stopped during observation

P(15515) = (39-8) / 39 = 0,8

P(15571) = 0,8 . (30-0) /30 = 0,8

Analogous

P(26514) = P(21023) = P(21481) = P(21841) = P(22000) = P(22130) = P(22715) = P(22850) = P(23522) = 0,8

P(23915) = 0,8. (22-1) :22 = 0,764

P(25393) = 0,764 . (19-1) : 19 = 0,723

P(25480) = P(25531) = P(25624) = P(25724) = P(26409) = 0,723

P(27303) = 0,723 . (13-1) : 13 = 0,668

P(27150) = P(27510) = P(29241) = P(30005) = P(30669) = P(32630) = 0,668

P(36800) = 0,668 . (15-2) : 5 = 0,441

- determining the probability of failure-free operation of the failed elements:

$\delta_1 = \delta_2 = \delta_3 = \delta_4 = \delta_5 = \delta_6 = \delta_7 = \delta_8 = 1 / (39+1) = 0{,}025$

P(10460) = 1 - 0,025 = 0,975 P(11153) = 0,975 - 0,025 = 0,975

P(11632) = 0,950 - 0,025 = 0,925 P(12016) = 0,925 - 0,025 = 0,900

P(12810) = 0,900 - 0,025 = 0,875 P(13642) = 0,875 - 0,025 = 0,850

P(13950) = 0,850 - 0,025 = 0,825 P(14119) = 0,825 - 0,025 = 0,800

δ_9 = 0,80 / (21+1) = 0,0364

δ_{10} = 0,764 / (19+1) = 0,038

δ_{11} = 0,726 / (12+1) = 0,0558

$\delta_{12} = \delta_{13}$ = 0,670 : (5+1) = 0,112

P(23602) = 0,800 - 0,0364 = 0,764 P(34330) = 0,670 - 0,112 = 0,558

P(24670) = 0,764 - 0,038 = 0,726 P(34610) = 0,558 - 0,112 = 0,446

P(26735) = 0,726 - 0,0558 = 0,670

The results obtained indicate that:

P(14119 ÷23552) ≥ 0,8 > P(23602)

$$T_{80\%} = 18820 + (23602 - 18820)\frac{(0{,}8 - 0{,}8)}{(0{,}8 - 0{,}764)} = 18820 \quad l \text{ - fuel}$$

80% - gamma resource of the main components and assemblies of forklifts

Table 5

№	Components and Assemblies	80% Gamma Resource	№	Components and Assemblies	80% Gamma Resource
1.	Engine	13 171	12.	Voltage Regulator	7 204
2.	Cylinder Head	18 820	13.	Starter	14 073
3.	Nozzle	7 742	14.	Hydraulic Pump.	17 014
4.	Fuel Pump	19 835	15.	Distributor	22 198
5.	Priming Pump	17 637	16.	Hydraulic Cylinder	29 480
6.	Oil Pump	29 560	17.	Steering Axle	19 498
7.	Water Pump	10 402	18.	Drive Axle	19 496
8.	Radiator	23 410	19.	Wheel Set	9 016
9.	Clutch	11 847	20.	Lifting Device	17 889
10.	Gearbox	14 368	21.	Battery	8 482
11.	Generator	12 250			

Conclusions

A methodological approach for determining the 80% gamma resource of forklift components has been proposed, considering both known and unknown resource distribution laws, as well as truncated and multiple-truncated sampling.

The 80% gamma resource has been calculated for the main components of forklifts. The obtained results can be used for planning the needs for spare parts to maintain the operational readiness of forklifts.

References

1. Tasev G., M. Mihov, Sv. Madzhov, Theoretical Foundations of Reliability - Avangard Prima Publishing, Sofia, 2022, p. 554.
2. Mihov M., Reliability of Machinery in Agriculture - Avangard Prima Publishing, Sofia, 2012, p. 178.
3. Tasev G., Methods for Restoring Worn-Out Parts - Sofia, 2009, p. 254.
4. Mihov M., Repair of Agricultural Machinery - Monograph, Avangard Prima Publishing, Sofia, 2019, p. 153.
5. Davchev Zh., M. Mihov, G. Tasev, Methodology for Testing Agricultural Machinery - Avangard Prima Publishing, Sofia, 2021, p. 302.

Characterization of lettuce germplasm (*Lactuca sativa* L.) stored in the Genetic Bank of Albania

Valbona Hobdari
Institute of Plant Genetic Resources, Agricultural University of Tirana, Tirana, Albania
vhobdari@ubt.edu.al

Abstract: *Lettuce is an important leafy vegetable for Albanians. It is mostly used as a fresh salad. There are several forms (species) of lettuce that are cultivated in Albania, but Albanian farmers cultivate and market mostly the farmer's cultivars (landraces), which are cultivars adapted to the conditions of the country and to the farming practice of the farmer. The introduction of foreign lettuce species increases the risk of genetic erosion of the farmer's cultivars. Through various projects, cultivars of the salad farmer have been collected and their seeds are stored in the country's Genetic Bank. This study was undertaken to recognize the morphological characteristics, as well as to evaluate the genetic variation of these genotypes with the aim of increasing the effectiveness of their using in possible genetic improvement programs, as well as other studies. In the study, 10 accessions (farmer cultivars) collected in different areas of Albania and stored in the Genetic Bank were taken.*

Keywords: *LETTUCE, LACTUCA SATIVA, FARMER'S CULTIVAR, LANDRACES, DESCRIPTOR, CHARACTERIZATION*

1. Introduction

Lettuce (*Lactuca sativa*) is the most important vegetable crop in the group of leafy vegetables [2, 3, 5]. The origin of lettuce is Europe, but it spread and was rapidly cultivated throughout the world [1]. It is a well-known plant worldwide due to its use in the preparation of salads, soups, etc. This plant is one of the oldest known edible vegetables and has gained importance mainly due to its biological activities, including antioxidant activity, antimicrobial activity and neuroprotective activity [5]. Lettuce includes seven main groups of cultivars (including oilseed lettuce) that differ phenotypically, and are usually described as morphotypes (morphological types) [3]. It is considered an important source of plant nutrients. This vegetable is rich in mineral nutrients such as vitamins, calcium, iron, flavonoids, fiber, potassium and phosphorus. It is a valuable dietary source of vitamin K, E and C, as well as carotenoids [5]. The chemical composition of the plant revealed the presence of different classes of secondary metabolites, such as terpenoids, flavonoids and phenols, which should be responsible for its biological activities. The plant also contains essential elements, such as vitamins, minerals and organic substances. It is characterized by significant morphological and genetic variations [3, 4].

This leafy vegetable plant was first cultivated by the Egyptians. Today, lettuce is produced all over the world and this plant has excellent medicinal properties. It is used in forensic medicine for many diseases, including pain, stomach and inflammation problems, as well as urinary tract infections. Various studies have provided scientific evidence of its pharmacological potential, including antimicrobial, antioxidant, neuroprotective and hypnotic effects [4]. Some of the benefits that lettuce offers to the human organism: Removes headaches and eases sleep; for these benefits, the lettuce is soaked in warm water, some fresh mint leaves are added and the drinks are taken before bed. It prevents Alzheimer's disease. It dissolves fats and helps to reduce weight. Fights body toxins and poisons. Fights cancer cells and prevents aging. It facilitates blood circulation and protects the heart. Protects bone health and prevents osteoporosis. The selenium contained in lettuce helps to strengthen the immune system. It lowers the body temperature and refreshes it. It is diuretic and facilitates metabolism and waste elimination. Important nutrient for pregnant women and regenerator of milk. Lowers blood pressure. Alleviates disorders in the large intestine. Fights anemia, strengthens the body, removes body odor. Strengthens vision and fights eye infections. Removes skin rashes and itching. It brightens the skin and prevents hair loss, because it stimulates blood circulation [1].

Lettuce is cultivated worldwide and is one of the most consumed green leafy vegetables in fresh (raw) form for its taste and high nutritional value [4]. Lettuce is grown on all continents, but the largest consumers and producers are the USA (91,000 hectares, of which 60,000 ha are in California) and Europe (the total area of the countries of the European Economic Community 80,000 ha). Large areas of lettuce are also grown in southeastern Australia, Japan, China, Israel, northern Mexico, Chile, Argentina, Brazil, and Peru [6]. Spain, China, USA, India, Japan and Italy are among the main producers in the world [2, 5]. China ranks first in the world for the cultivation of lettuce, followed by the USA and India. In Albania, it is also called green salad and is widely used in the kitchen [1]. Lettuce is very important as a commercial crop in North and Central America, Asia and Europe [5].

In general, the morphological and agronomic description of wild lettuce accessions is not complete. Even the status of some species related to cultivated lettuce is not detailed. In lettuce, morphological studies have been carried out in Slovenian and Swedish, Austrian and Italian, Brazilian, Philippine and Iranian genetic resources [5].

Genetic improvement of lettuce is mainly focused on different morphological characteristics and resistance to diseases and pests. Accurate lettuce germplasm descriptors provide useful basic information for breeders. The compilation of the list of lettuce descriptors has been stimulated by the international gene bank community [2]. This list consists of 55 descriptors with 15 of them illustrated with pictures. It provides the means for the detailed characterization and differentiation within intraspecific variation of L. sativa, for the verification of old varieties and for the identification of releases and putative gaps in germplasm collections. These descriptors, together with the descriptors of wild Lactuca species, provide the efficient analytical tool for studying the complex morphological variability of this genus and the relationships between species [3, 2]. Genetic improvement of lettuce is mainly focused on different morphological characteristics and resistance to diseases and pests. Accurate lettuce germplasm descriptors provide useful basic information for breeders. The compilation of the list of lettuce descriptors has been stimulated by the international gene bank community [2]. This list consists of 55 descriptors with 15 of them illustrated with pictures. It provides the means for the detailed characterization and differentiation within intraspecific variation of L. sativa, for the verification of old varieties and for the identification of releases and putative gaps in germplasm collections. These descriptors, together with the descriptors of wild Lactuca species, provide the efficient analytical tool for studying the complex morphological variability of this genus and the relationships between species [3, 2].

The Institute of Genetic Resources in Albania, within its mission, has collected preserves, regenerates, characterizes and evaluates the genetic material of the cultivated lettuce (Lactuca sativa L) collection [2].

2. The purpose of the study

The purpose of the study was to know the morphological characteristics and qualitative features of the accessions of Albanian lettuce, which are stored in the Albanian Genetic Bank.

3. Objectives of the study

The objective of the study was the characterization of lettuce accessions, i.e. the evaluation, recording and recognition of morphological characteristics with the aim of highlighting the

morphological diversity among lettuce accessions, collected locally and stored in the Genetic Bank to enable their more efficient use effectiveness by researchers and crop genetic improvers.

4. Materials and methods

Materials used in the study

In the study, 10 accessions of lettuce (*Lactuca sativa* L.) representing the farmer's cultivars (landrace) were taken, which collected in 6 districts of the country, are stored in the Albanian Genetic Bank.

The study was conducted at the Experimental Base of the Genetic Bank near the EDE of the Agricultural University of Tirana, in Valias [longitude 19043'59.90"E; latitude 41024'04.30"N; altitude 39 m]. The establishment of the field trial was based on international standards (FAO, 2014. Genebank standards for leafy vegetables) and the assessments for the characterization of the genetic material were based on the minimal descriptors (ECPGR, 2009 and IBPGR Secretariat, Rome, 1996). The accessions used for the study are part of the germplasm collections kept in the Genetic Bank of Albania.

Table no. 1: Lettuce farmer's cultivars and collection points

No. of accession	Accession name	Site of collection
AGB3807	Sallatë marule e Piskovës	Përmet
AGB3878	Sallatë marule e Bulgarecit	Korçë
AGB4169	Sallatë marule e Mirasit	Korçë
AGB4170	Sallatë vendi e Lushnjes	Lushnje
AGB4171	Sallatë marule e Korçës	Korçë
AGB4172	Sallatë vendi e Fierit	Fier
AGB4173	Sallatë e Berdicës	Shkodër
AGB4174	Sallatë Bari vendi	Përmet
AGB4175	Sallatë e Leshnicës	Përmet
AGB4180	Sallatë Allias-78	Tiranë

Planting was done on March 16, 2022 in polystyrene trays with 170 cells, with a cell diameter of 4.2 cm, filled with Flora Gard soil. Seeds germinated on March 24–26, 2022. Seedlings were planted in the field on April 21, 2022. The experimental design was randomized block with three replications. Each variant in the replicate was represented by 30 plants, planted in three rows of 4.0 m length, with 10 plants per row. The distance between rows was 60 cm and between plants in rows 40 cm. planting density was 4.16 plants/m^2. So, the variant in each replication had an area of 7.2 m2.

During the growing season, all the agro technical services performed on the lettuce plant in production were carried out; care was taken to water once every 2–3 days until the flowering period and, later, during the flowering and fruit-setting period, the plants were watered every day. Field observations were made for the field trial condition and germination, flowering and ripening dates were recorded for each accession.

5. Results and discussion

The characterization of lettuce accessions was carried out through the descriptors of the morphological characteristics of the leaf, flower, head and achene of lettuce.

Let's first elaborate on the variation of lettuce accessions via leaf descriptors. Several leaf morphological characteristics were analyzed but 9 descriptors were recorded on which we are examining the variation among the lettuce accessions under study.

a. Genetic variation of lettuce accessions according to leaf morphological characteristics

The shape of the adult leaf showed wide variation, all 10 accessions in the study were divided into 5 groups, of which 3 accessions had broad elliptic leaves, 1 was elliptic, and the other 6 had leaves of other shapes (table no. 2).

The base of the leaf is expressed in two forms, from the three classes that this descriptor has in total; 6 accessions had the leaf with a short attenuate base, while the other 4 had a medium attenuate base, so this feature has good variation (table no. 2).

Table no. 2: Descriptors of lettuce accessions

Lettuce accessories		Number of accessions
Descriptor number and name	Status	
1.3.7.1 Outer adult leaf-entire-shape of blade in outline	**2**	**1**
	3	**3**
	4	**2**
	6	**2**
	7	**2**
1.3.10 Outer adult leaf-shape of blade base	**1**	**6**
	2	**4**
1.3.9 Outer adult leaf-shape of apex	**1**	**2**
	2	**8**
1.3.7.2 Outer adult leaf-entire-margin of blade	**1**	**2**
	3	**8**
1.3.5 Outer adult leaf-surface profile	**1**	**9**
	2	**1**
1.3.11 Outer adult leaf-blistering	**0**	**1**
	3	**4**
	5	**5**
1.3.1 Outer adult leaf-colour	**1**	**2**
	2	**7**
	5	**1**
1.3.2 Outer adult leaf-intensity of colour	**5**	**9**
	7	**1**
1.3.3.1 Outer adult leaf-anthocyanin-distribution	**0**	**9**
	1	**1**
1.6.1 Flower-colour of ligule	**5**	**10**
1.6.2.1 Flower-anthocyanin-distribution pattern on lower part of ligule	**0**	**9**
	2	**1**
1.4.1 Head-formation	**0**	**1**
	1	**9**
1.4.4.1 Head-shape in vertical section	**3**	**5**
	4	**4**
1.4.4.3 Head-firmness	**5**	**9**
1.4.4.2 Head-overlapping of leaves	**3**	**5**
	5	**4**
1.4.5 Leaf rosette position of leaves	**1**	**1**
	7	**9**
1.7.1 Achene-colour	**2**	**7**
	7	**3**

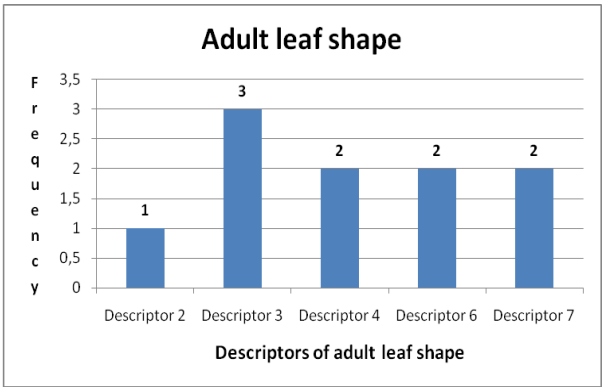


Chart no. 1: *Frequency of lettuce accessions according to the adult leaf shape*

As for the shape of the apex of the leaves, the leaf with a rounded tip prevails, which includes 8 accessions; only two accessions have truncate leaf tips (table no. 2).

For the margin of the blade leaf, accessions with dentate sides predominate (8 accessions), while the other two have entire leaves. So even for this feature there is variation between accessions.

Farmer's cultivars of the lettuce also showed variation for the appearance of the leaf surface, for this feature the accessions with concave (spoon) leaves predominate where 9 accessions belong, only one accession had flat leaves.

Blisters can also form on lettuce leaves, which depend on the cultivar, so the appearance of blisters is controlled by genetic factors. For this feature, lettuce accessions are divided into 3 groups (table no. 2), out of 4 groups that this descriptor has in total; so this trait showed good variation. Thus, for example, 1 accession (Sallata e Bërdicës) has the surface of the outer adult leaf without any bubbles (grade 0), 4 accessions (Marule e Bulgarecit, Marule e Mirasit, Sallata e Lushnjes and Sallata e Fierit) had slight blistering (grade 3) and the other 5 accessions had moderate blistering (grade 5).

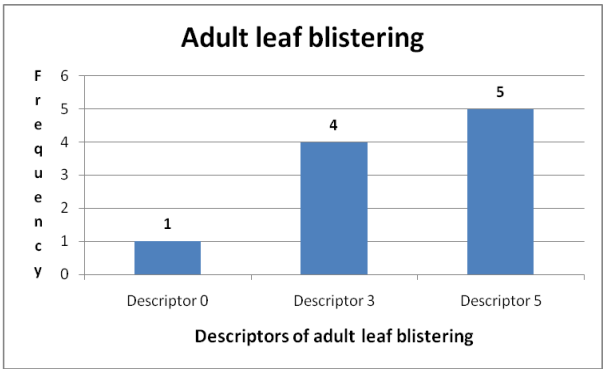


Chart no. 2: *Frequency of lettuce accessions according to adult leaf blistering*

The green color (class 2) of the outer adult leaf-colour appeared in most accessions (7 accessions), 2 accessions and (Marule e Bulgarecit and Marule e Korçës) have green to yellow leaves (descriptor 1), while one accession "Sallata e Leshnicës" has red and green colored leaves (table no. 2).

Regarding the intensity of leaf color, the lettuce accessions in the study mostly showed moderate intensity of leaf color (class 5); while one accessory (Sallata marule e Mirasit) has an intense green color (grade 7).

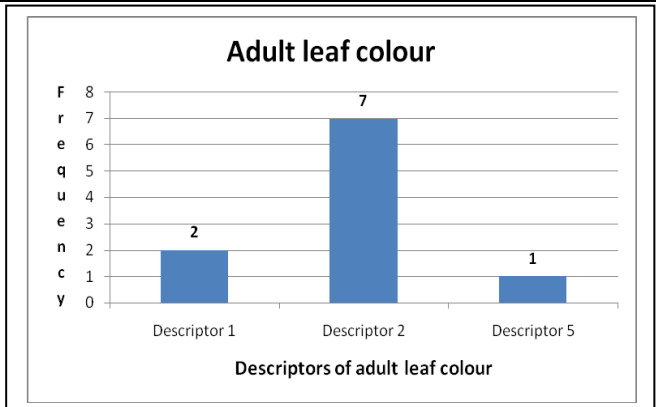


Chart no. 3: *Frequency of lettuce accessions according to adult leaf colour*

The appearance of anthocyanin on the leaves is interesting. For this descriptor, most accessions (9 accessions) had no anthocyanin on the leaves, only one accession (Sallata e Leshnicës) had anthocyanin only on the veins (grade 1).

b. Genetic variation of lettuce accessions according to flower morphological characteristics.

The lettuce accessions did not show variation regarding the color of the flower crown, all 10 accessions formed flowers with a yellow crown (grade 5).

Regarding the distribution of anthocyanin on the flowers, 9 accessions did not have anthocyanin on the flowers (*grade* 0), only one accession (Sallata e Leshnic*ës*) has anthocyanin on the *margin* of the flower (grade 2).

c. Genetic variation of lettuce accessions according to head morphological characteristics.

For morphological characteristics, we assessed and recorded 6 descriptors. Let's examine each of them in turn.

Regarding the formation of the head, the lettuce accessions are divided into two classes of the descriptor, but 9 of them formed a head, that is, they are var.capitata, the only exception was "Sallata e Bërdicës", which did not form a head (table no. 2) . In terms of head shape in vertical section, five lettuce accessions form broad elliptic heads (grade 3), while the other four form orbicular heads (grade 4).

Regarding the firmness of the head, all 9 accessions that formed a head were evaluated with medium firmness of the head (grade 5).

Regarding the overlap of the head leaves, the lettuce accessions are divided into two groups, of which 5 accessions were assessed as partly covered (class 3) and 4 accessions with half-covered heads (grade 5)

For the position of the leaves, i.e. for the angle that the leaves of the rosette form with the horizontal plane, in 1 accession (Sallata e Bërdicës), which does not form a head, the position of the leaves of the rosette is very upright (grade 1). In other accessions, which form a head, the position of the leaves of the rosette with the horizontal plane is assessed as flat (grade 7).

d. Genetic variation of lettuce accessions according to seed morphological characteristics.

As for the color of the achene, it can be said that there is an interesting diversity: three accessions (Sallatë vendi e Lushnjes, Sallatë vendi e Fierit and Sallata e Bërdicës) have black colored achenes; all the others have white to gray color.

6. CONCLUSION

Based on the data of the study and their review and discussion, we draw some conclusions.

1. The germplasm of 10 accessions of country lettuce was characterized by wide variation for the outer adult leaf-shape of blade in outline, all 10 accessions were divided into 5 groups;
2. Even for the base of the leaf good variation was shown, the accessions were grouped into two classes out of the three that this descriptor has in total. Even for the outer adult leaf-shape of apex, lettuce accessions expressed variation;
3. For the color of the outer adult leaf, the farmers cultivars of the lettuce were divided into three classes in which the green color prevailed, which was in 70.0% of the accessions;
4. For the color of the flower, all the accessions had only the yellow color, so for this descriptor there was no variation;
5. For head formation, only one accession did not form a head, while the other 9 (90 %) did form a head;
6. For achene color, the lettuce accessions were divided into two groups, of which 3 accessions had black achene, while the other 7 had white to gray achene.
7. We consider the information obtained from this study to be useful for the genetic variation of lettuce stored in the Albanian Genetic Bank;
8. This variation in the characterization of lettuce accessions may also be important for use in genetic improvement programs of this plant.

7. REFERENCAT

1. Beta E. (2016). Konsumoni marule (sallatë jeshile)? Ja çfarë nuk dini për të! Healthyfood;
7. Jani S. (2022). Për studimin "Karakterizimi morfologjik dhe vlerësimin e disa acc të germplazmës së sallatës (*Lactuca sativa* L.)", 2022. Raport. Instituti i Resurseve Gjenetike të Bimëve.
3. Křístková E., Doležalová I., Lebeda A., Vinter V., Novotná A. (2008). Description of morphological characters of lettuce (*Lactuca sativa* L.) genetic resources. Hort. Sci. (Prague), 35, 2008 (3): 113–129;
4. Kuete V. (2017). Medicinal Spices and Vegetables from Africa; therapeutic potencial against metabolic, inflamatore, infectious and systemic diseases. Amsterdam: Academic Press (2017);
5.Lallouche Bahia, Hadj Kouider Boubakr, Beloudah Asma, Ben Madani Reguia and Boutekrabt Ammar (2020). Phenotypic characterization of some lettuce cultivars (*Lactuca sativa* L.) cultivated in Algeria. Revue Agrobiologia (2020) 10(1): 1787-96;
6.Pink D.A.C., Keane Evan M. (1993). Genetic Improvement of Vegetable Crops. 40-Lettuce: *Lactuca sativa* L. Available online 2 December 2012.